6 Hydrological Data Analysis and Modelling

The goal of the hydrological data analysis is the estimation of water availability and its reliability. At first, the Ta'izz rainfall data are analysed in different time scales: year, day and decade. The annual data offer a general climatic picture, the daily time step is the original time scale of the data and the 10-day interval the actual scale that is used for the reliability analysis.

Due to their quality, the data had to be checked thoroughly. For all data distribution, independence, periodicity and trend were investigated and further tests of data consistency were necessary. The basic statistical investigation and interpretation was done set by set. Only then further processing was conducted.

The field data of Mia'amirah are more diverse. Beside the climatic data, which are processed analogue to the Ta'izz data, geomorphological information is analysed to provide information on the hydrological characteristics of the terraces. Those data are supplied to the precipitation – evaporation model that evaluates the different geomorphological components of the catchment. The results are discussed in chapter 6.3.2.

6.1 Analysis of the Ta'izz Precipitation Data

6.1.1 Annual Data

The annual data were compiled from different sources. They present different measurement locations within Ta'izz. The data were provided by NWRA. Due to the geographical location of Ta'izz on the foot of Jabal Sabir, the locations have a significant range in altitude. On the other hand, they represent the longest time series (1944-1995). They were used only for the determination of the precipitation regime.

The histogram of the annual precipitation (figure 6.1) shows a unimodal distribution that meets the conditions of the normal distribution, although the Pearson correlation coefficient between the empirical and theoretical distribution is only 0.78 (*Chi-Test*: $\chi^2 = 4.7 \; < \; \hat{\chi}^2_{\phi=9,\alpha=0.05} = 16.25$). The lag-plot of year *i* to year *i-1* in figure 6.2 shows no persistence from year to year.

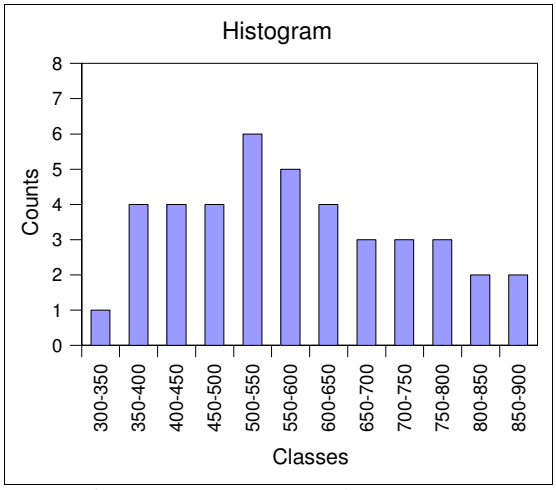

Figure 6.1 Histogram of annual precipitation

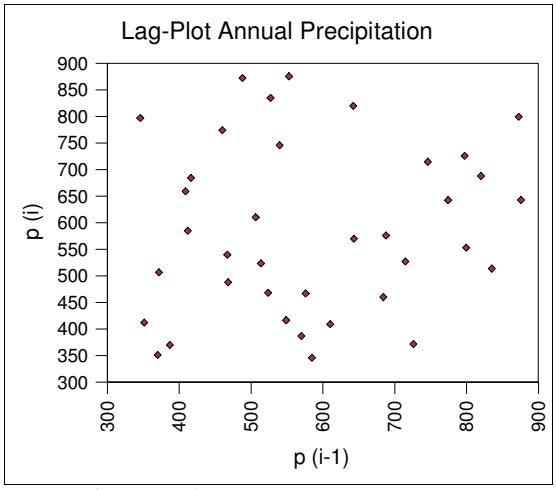

Figure 6.2 Lag-plot of annual precipitation

6.1.2 Annual Precipitation Regime

An overview over the basic statistic numbers is given in table 6.1. The annual precipitation of the examined period ranges between 346.0 mm and 875.8 mm, and the standard deviation reaches with 153.1 mm a little less than 25% of the mean precipitation of 584.2 mm. The latter is considerably smaller than the mean potential evaporation of 1640 mm (BRUGGEMAN 1997).

The definition of dry – or drought – years is laborious and depends much on the circumstances. DEMUTH and STAHL (2001) suggest the 80 % percentile (P80) as a threshold for a meteorological drought for monthly data while they use P70, P80, P90 for drought estimation on annual basis. HASTENRATH and HELLER (1977) chose a different method to access rainfall patterns in the Sertão, NE Brazil. They expressed the annual precipitation in terms of standard deviation ('normalised departure') as shown in figure 6.4 for the Ta'izz data.[53] Starting from such a graph and additional runoff data they classified "dry" years by a threshold of -0.5σ, and "wet" years by 0.7σ. "Extreme"

Table 6.1 Annual precipitation, basic statisics

Parameter	***Value***
mean	584.2
median	570.1
min	346.0
max	875.8
range	529.8
stdev	153.1
variance	23440.94
skew	0.28
kurtosis	-0.92

53 Normalising was done in order to make the time series comparable.

in both directions was defined as ±0.5σ, "very extreme" as ±1.2σ. These thresholds are indicated by dashed lines in figure 6.4. For the Ta'izz region, no sufficient runoff data are available and the direct transfer of the threshold should be done with special care. For both methods, it has to be considered that statistical definitions of drought do not take into account natural and human water demand. Therefore, this kind of definition needs to be empirically examined or otherwise justified. If not no conclusion can be drawn. However, for the statistical assessment of the precipitation regime this approach offers some help and makes the result comparable to other data.

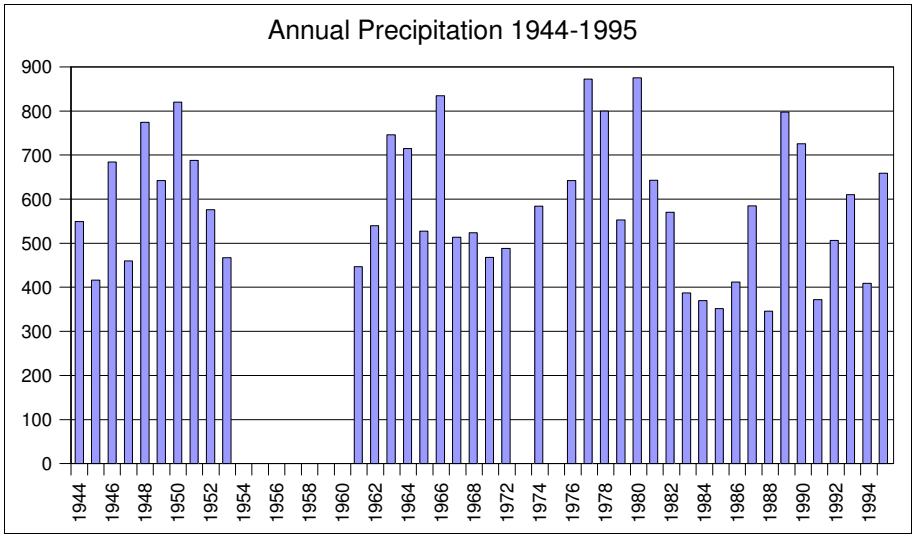

Figure 6.3 Annual precipitation 1944-1995 (years 1954-1960, 1969, 1973, 1975 missing)

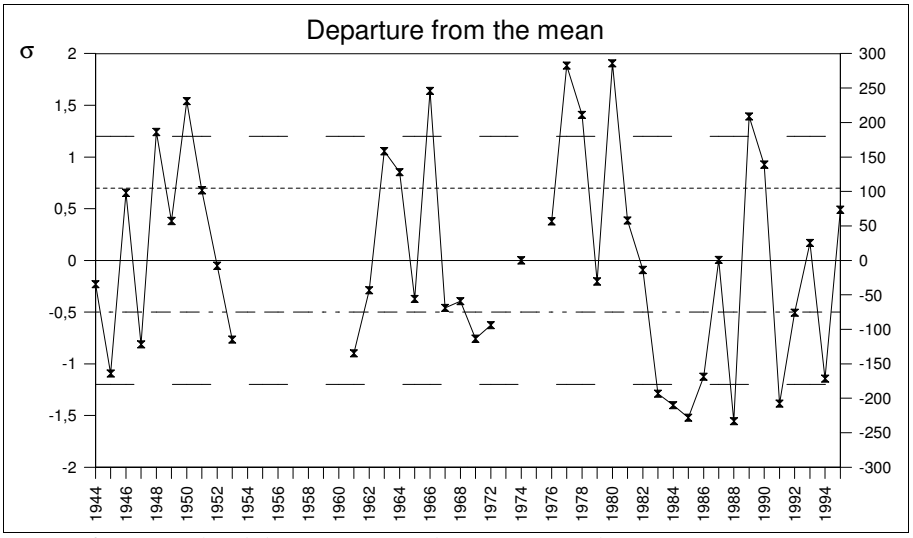

Figure 6.4 Normalised departure from the mean annual precipitation

Applied to the Ta'izz time series, the -0.5σ threshold equals an annual precipitation of 508 mm which is one third of the potential evapotranspiration of 1640 mm. 508 mm of rainfall are still considerably more than the average rainfall in most of the other places in Yemen. The -1.2σ threshold equals an annual precipitation of 400 mm. Nevertheless, figure 6.4 depicts the high inter-annual variation of the rainfall. The 80 % percentile corresponds with an annual precipitation of 446 mm (or 0.9σ) (see figure 6.3) which was accepted as a reasonable estimation. Using the P80 for drought definition, 9 of 41 years or 22 % were considered dry.

The plotting positions of the exceedance probability are shown in figure 6.5. The Weibull, Hazen and Gringorten formulas are used alternatively. Apart from the recurrence interval the differences are neglectable. For the Ta'izz annual rainfall series 1944-1995 the sum of squared deviation is given in table 6.2. It indicates that the difference between the formulas is not relevant.

Table 6.2 Sum and mean of squared deviation of Ta'izz annual precipitation 1944-1995

Name	***Sum of Squared Deviation***	***Mean Squared Deviation***	***Pearson Correlation Coefficient***
Weibull vs. Hazen	0.00194	0.000047	1.000
Weibull vs. Gringorten	0.00679	0.000166	1.000

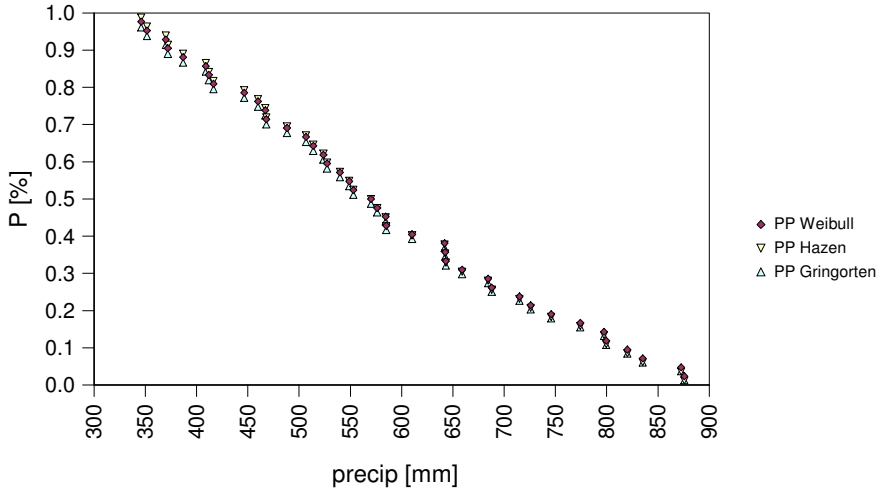

Figure 6.5 Plotting positions annual exceedance probability of precipitation, Ta'izz

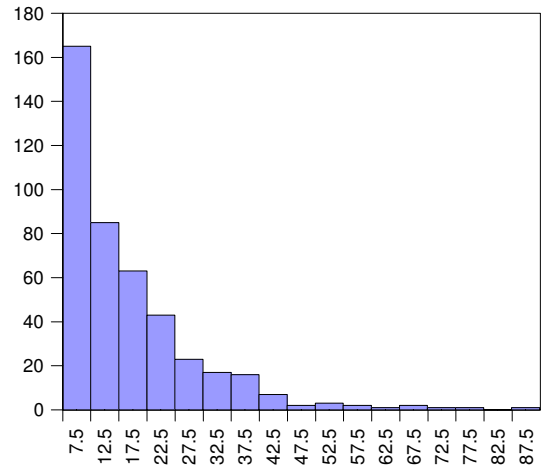

Figure 6.6 Frequency distribution of daily precipitation > 5 mm

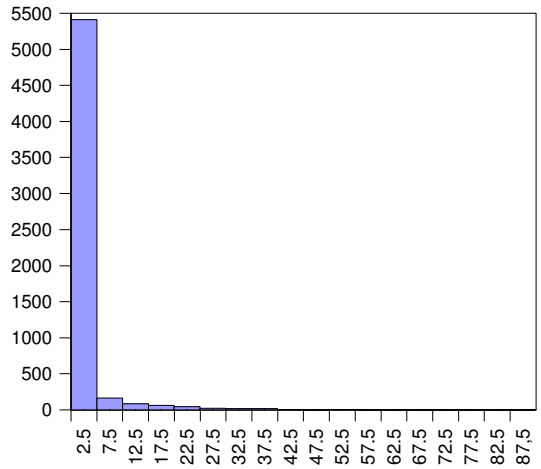

Figure 6.7 Frequency distribution of daily precipitation with 0

6.1.3 Daily Data

The daily precipitation data are provided by the AREA office branche Ta'izz who operate the meteorological station on their research farm in Osiferah (latitude: 13°36', longitude 44°01', altitude 1400 m a.s.l.), a quarter in the lower part of Ta'izz. They are divided into 2 sets (1990-1991, 1995-1998). The gap was caused by confusion and civil war upon the reunification of the South Yemen (PDRY) and Yemen Arab Republik (YAR) to the Yemen Republic on May 22, 1990. The station is operated manually, the readings usually are done in the morning. The maintenance of the station was poor.

The time series of the daily precipitation is strongly influenced by the dry season. In the frequency distribution 93 % of all counts fall in the class of 0-5 mm of precipitation (figure 6.7). For the analysis of time series the data have to remain unchanged, but for the analysis of rainfall events only "real" events > 0 were considered. Nevertheless, the frequency distribution just meets the criteria of the exponential distribution. With the Wilcoxon Rank-Sum Test the empirical distribution was tested against the theoretical exponential distribution. The computed probability ($p = 0.061$) is a little higher than the significance level ($\alpha = 0.05$). Therefore the hypothesis H0 can be accepted, the distribution is an exponential distribution. But it is worth mentioning that the probability exceeds the significance level only very little and we can assume that the adaptation is poor. The result is much better if the data collection is limited to precipitation higher than 5 mm (figure

6.6). The histogram shows a clear exponential pattern which is approved by the probability calculated with Wilcoxon Rank-Sum test : p = 0.214 (α = 0.05).

Table 6.3 Iteration test (Wallis and Moore) on data independence

Iteration test		
Hypothesis:	H0	independence
	A1	dependency
	significance level	0.05
Resultes:	**80-91**	**95-98**
z	76.59	41.08
probability:	0.00	0.00

Persistence is tested by auto-correlation and the iteration test of WALLIS and MOORE.[54] Due to the time gap of the years 1992-1994, the series 1980-1991 and 1995-1998 are tested separately. The autocorrelation shows in figure 6.8 that the daily values have no persistence. The iteration test shows the opposite result. The test rejects the H0 hypothesis (independence) and accepts the A1 (dependency). It is assumed that this test is affected by the type I error.[55] As a non-parametric test it proves the altering of the sign which is biased by the long dry period where zero follows after zero. For the daily precipitation data, the gradient of the regression line is 0,0000537, therefore no trend is assumed.

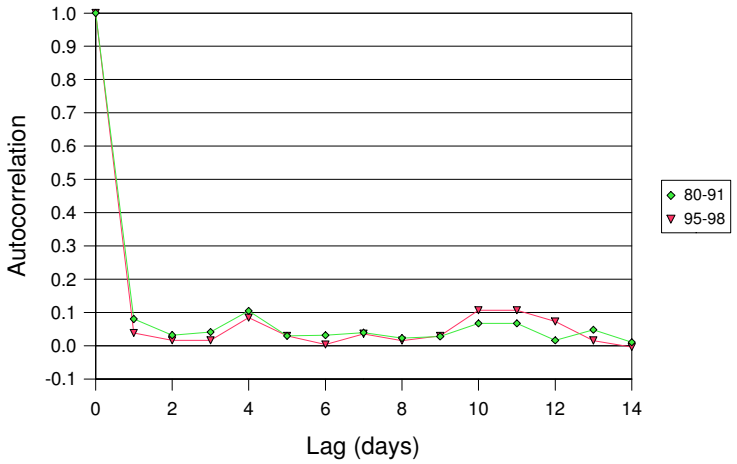

Figure 6.8 Autocorrelation of daily rainfall

6.1.3.1 Data Inconsistencies

The raw data show some inconsistencies including frequent gaps on weekends. To prove if the effect is significant it was tested if the mean precipitation was equally distributed on the days of the week. This was not the case, table 6.4 shows the result of the sample mean test which indicates that on Thursdays there is significantly less rainfall. Since the reading of precipitation was done after the precipitation, it is assumed that the reading on Fridays was not always done. Consequently, it can be assumed that the

54 in: SCHÖNWIESE (1992)
55 Type I error: Hypothesis H0 is rejected in case where H0 is true.

Thursday events are included in the Friday events. This assumption is supported by the fact that Fridays' mean precipitation is the highest of all, although the deviation does not reach a level of significance.

This test indicates that the precipitation data of the station Ta'izz Osiferah are of limited quality and reliability. Due to inconsistency of the daily data, analysis of the daily data is not suggested. Aggregation to 10-day intervals can reduce the error of infrequent data reading.

Table 6.4 Sample mean test to prove daily consistency

Day	***Count***	***Mean***	***Stdev***	***Z***	***Probability α=0.05***	***Result***
Sa	118	10.41	10.23	1.66	0.82	not sig
So	109	11.88	12.36	1.66	0.59	not sig
Mo	110	12.1	11.89	1.66	0.81	not sig
Tu	105	10.62	11.16	1.66	0.51	not sig
We	103	11.97	13.82	1.66	0.58	not sig
Th	87	7.87	6.85	1.66	**4.51**	**sig**
Fr	117	12.73	13.68	1.66	1.23	not sig

6.1.3.2 Decades

Similarly to the daily data, the frequency distribution of the 10-day sums in figure 6.9 emphasis the dry season. More than 50 % of the decades belong to the class 0-5 mm. The distribution exactly meets the exponential condition (Z= -1.582, p = 0.056).

The autocorrelation in figure 6.10 suggests a small short term persistence (lag =1). Clearly to recognise is the annual pattern (lag ≃ 36). The lag-plot, which is more rigorous, shows no persistence (figure 6.11). The trend was tested with the Mann-Kendall test (M-K test).[56]

Table 6.5 Mann-Kendall test statistics

M-K test	***alpha = 0.05***
τ correlation	0.1
S	22.0
z	1.006
p	0.3146

56 see: HELSEL et al. (1992), SALAS (1993)

The M-K statistics is given in table 6.5 and indicates no trend at $\alpha = 0.05$ significance level. The confirmatory statistics show that the data are not normally distributed, have no persistence and no trend.

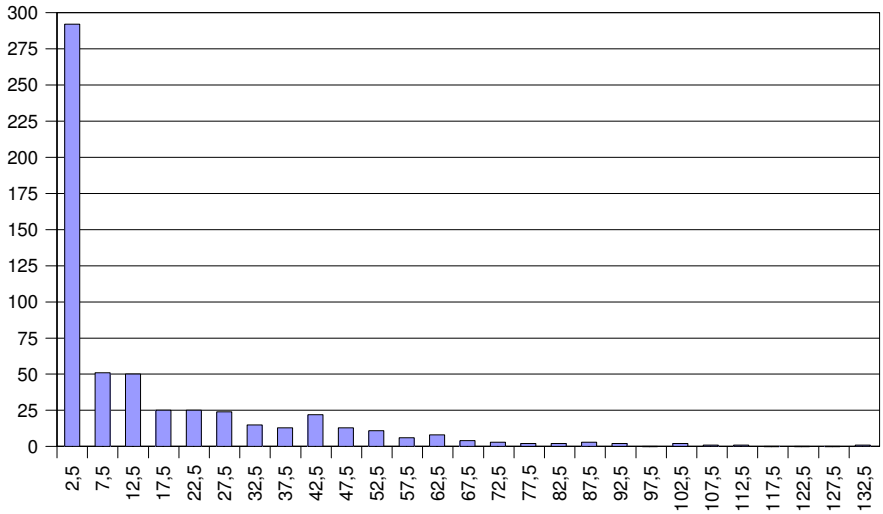

Figure 6.9 Frequency distribution of decade precipitation

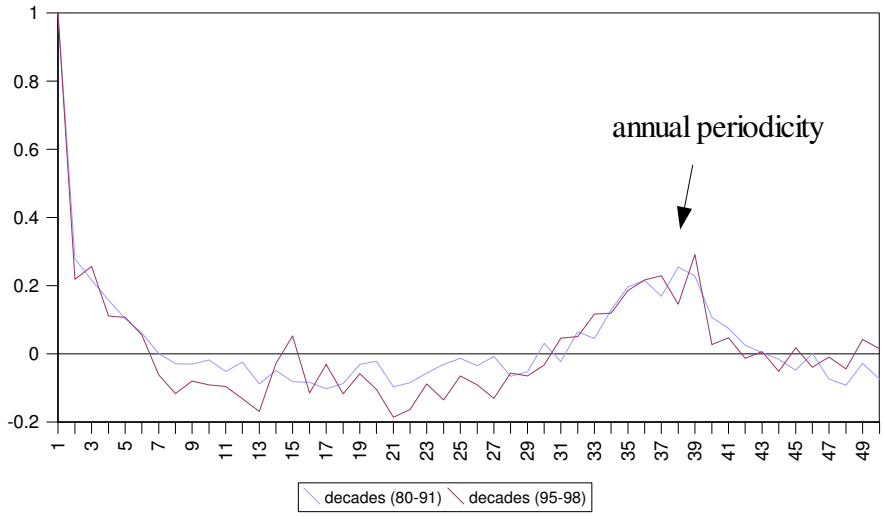

Figure 6.10 Autocorrelation of the decades (1980-1991, 1995-1998)

Figure 6.12 shows decade-sums of precipitation (mean precipitation of the years 1980-1991) and its standard deviation over the year. Significant precipitation occurs from the last decade in March until the first decade in October. The seasonal distribution shows a bimodal pattern. But the first peak is weakly developed and there is no clear intermediate dry season as known from other regions in Yemen (e.g. Sana'a, Mahwit).

The second rainy season from the last decade in August increases precipitation significantly until the first decade in October. From the 1st to the 2nd decade in October it plunges sharply. The standard deviation lies in the same range or higher than the mean precipitation. Hence, the inter-annual variation is quite high. The standard deviation

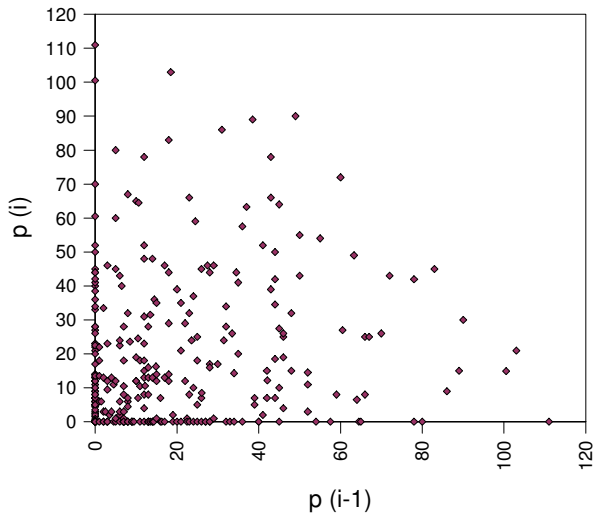

Figure 6.11 Lag plot decades (1980–1991)

reaches its peak at the beginning and end of the rainy season. This seems logical because the beginning and the end vary in time and this effect produces more variation. Still it is noteworthy how abruptly the rainy season start or ends. The precipitation stays in almost every decade below the reference evaporation (30-40 mm/decade). This important threshold is only exceeded in the 2nd rainy season.

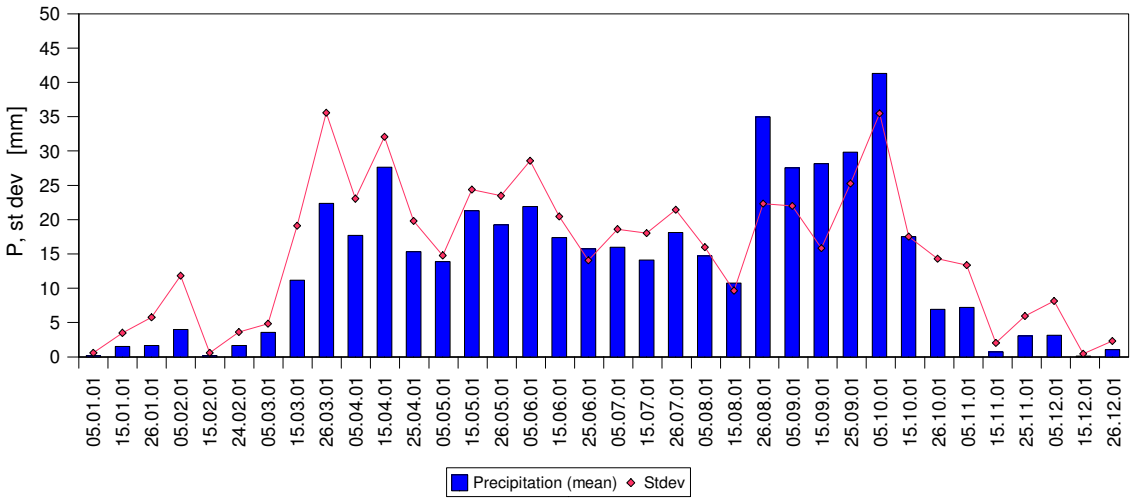

Figure 6.12 Mean precipitation (decades) and standard deviation

6.1.4 Plotting Positions, Exceedance Probability and Fitting of the Cumulative Density Function of Decade Precipitation Data

The plotting positions and the fitting of the theoretical distribution were computed as described in chapter 3.2. The decades 8 to 29, which cover the vegetation season, were used. Outside this period the fitting was not recommended due to the lack of precipitation events. All fittings are good, the Pearson correlation coefficient between empirical and theoretical probability is better than 0.9 for all decades of the rainy season. Outside the rainy season the correlation coefficient drops to values between 0.45 and 0.75.

Figure 6.13 shows the plotting positions and the fitted distributions. The decades 8-10 represent dry season conditions. In this case, for many years the precipitation is 0 and the fit is low. Substantial improvement starts from the 13th decade and lasts until the 29th. The plotting positions and the shape of the Weibull-CDF of the two rainy seasons differ from each other. The first rainy season begins with the 9th decade and lasts until the 15th decade. The 2nd rainy season starts with the 24th decade and lasts until the 28th decade.

The general shape of the Weibull-CDF in the first rainy season is more smoothly curved. In the second rainy season the CDF-curve has a more linear shape which might have a significant blip (e. g. decade 27). This shape leads to a different behaviour of the statistical model discussed below.

Knowing α and k of the CDF for individual decades it is possible to calculate the exceedance probability of a given amount of rainfall for every decade.[57] As an example, the probability of the mean precipitation is shown in figure 6.14.

The graph shows the mean precipitation (1st y-axis) and the exceedance probability of the mean precipitation (2nd y-axis) for the period from March 10th until the November20th. The precipitation shows a moderate peak (28 mm/decade) in March/April followed by a low at the end of April, beginning of May. In mid-May precipitation exceeds the 20 mm threshold again from where it constantly diminishes until mid-August. In the last decade of August the rainfall rises sharply from 20 mm/decade to 35 mm/decade and reaches the peak of 43 mm/decade at the end of the 2nd rainy season in the beginning of October. In the 2nd decade of October rainfall plunges rapidly which indicates the termination of the rainy season. The last decade of October already receives less than 10 mm/decade rainfall.

The probability of the mean precipitation follows a different pattern. At the start of the first rainy season in March/April the probability increases with a delay of one decade. But it rises only slightly above the level of 0.35! At this level it remains almost constant until the last decade of July except for a significant peak (0.46) in the end of June. For the 2nd rainy season the probability increases considerably and reaches its maximum of 0.49 in

57 Exceedance probability = 1- non-exceedance probability

mid-September. For the last decade in September the probability comes to an extreme low (0.19). This extreme deviation from the neighbouring values is interpreted by the author as an error in the primary data which could not be revealed.

In every decade the exceedance probability of the average rainfall remains below 0.5. The average probability is 0.36 which results in an recurrence interval of approximately 3 years for the "average year". The periode mid-August until the 1st decade of October has beside the highest precipitation also the highest reliability. This corresponds with the local experience that the 2nd rainy season in Ta'izz is generally considered the more important one. Overall, it can be concluded that the exceedance probability of the average precipitation is considerably low (< 0.5), which leads to the (generally known) conclusion that mean values do not represent semi-arid climate adequately. For rainfed agriculture a specific amount of precipitation (approx. 0.7 of ET_0[58]) is needed during the vegetation period with a high reliability. This can roughly be estimated at 25 mm/decade. Figure 6.14 shows that for the average year these conditions are only given for a short period during the 2nd rainy season. Hence, this simple estimation points out that rainfed agriculture cannot be the prevailing farming type under such conditions and supplementary irrigation is essential. A more thorough discussion in the context of water harvesting schemes will be given below.

58 Definition of growing period used by Bruggeman (1997).

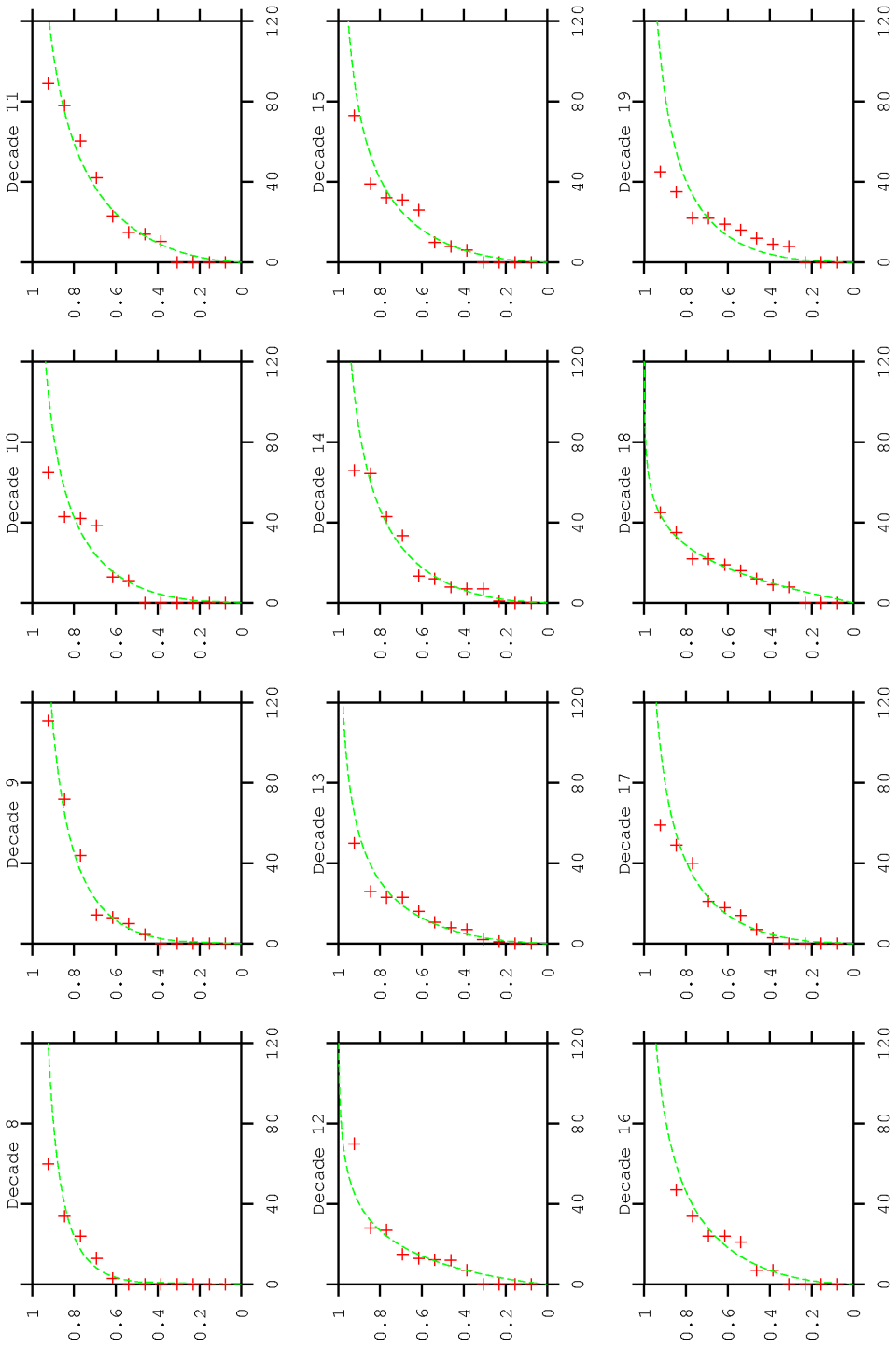

Figure 6.13 Plotting positions of non-exceedance probablilty and fitted Weibull CDF

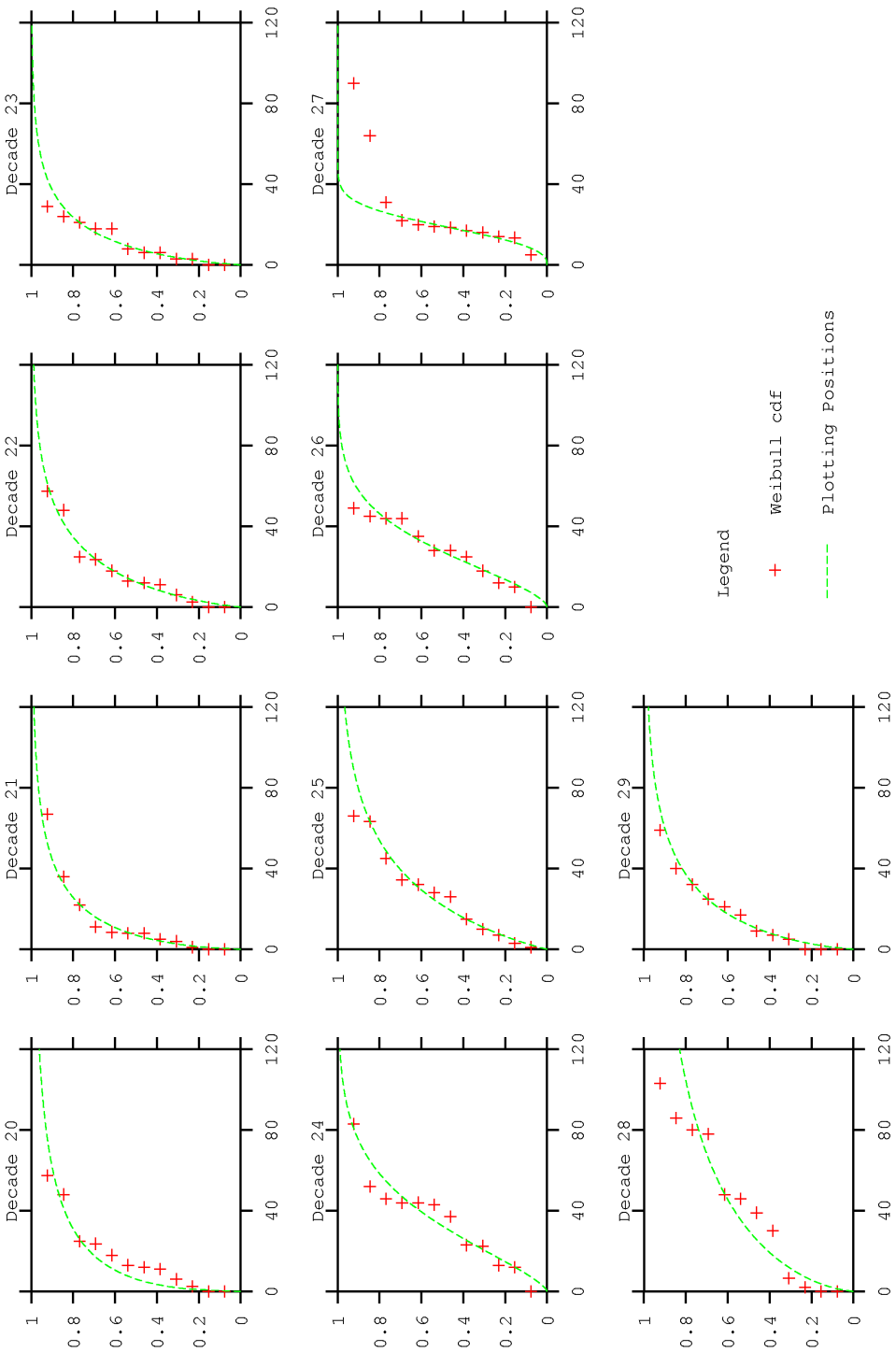

Figure 6.13 (cont.) Plotting positions of non-exceedance probablilty and fitted Weibull CDF

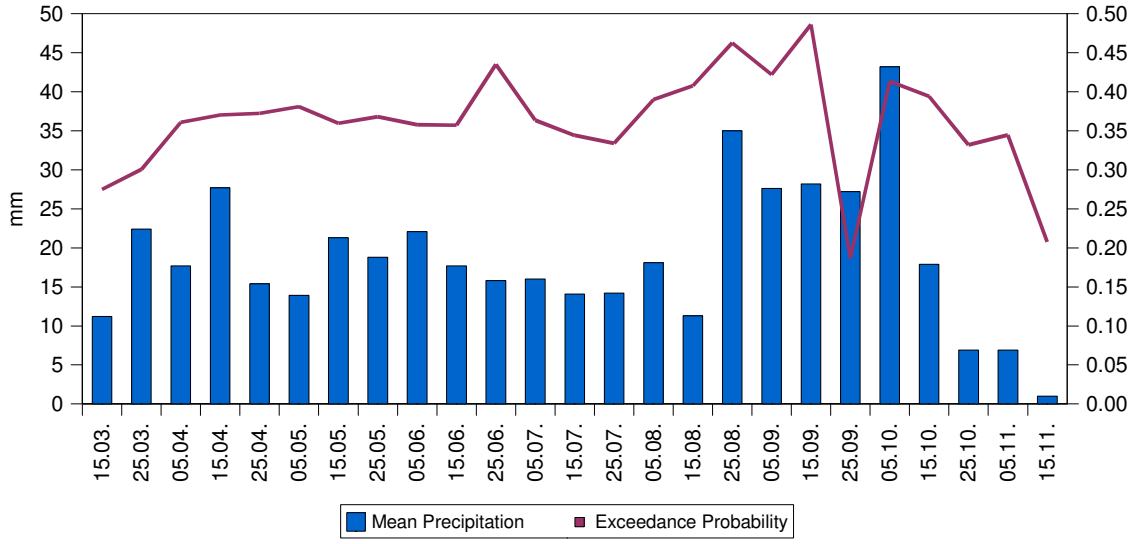

Figure 6.14 Mean precipitation and its exceedance probability

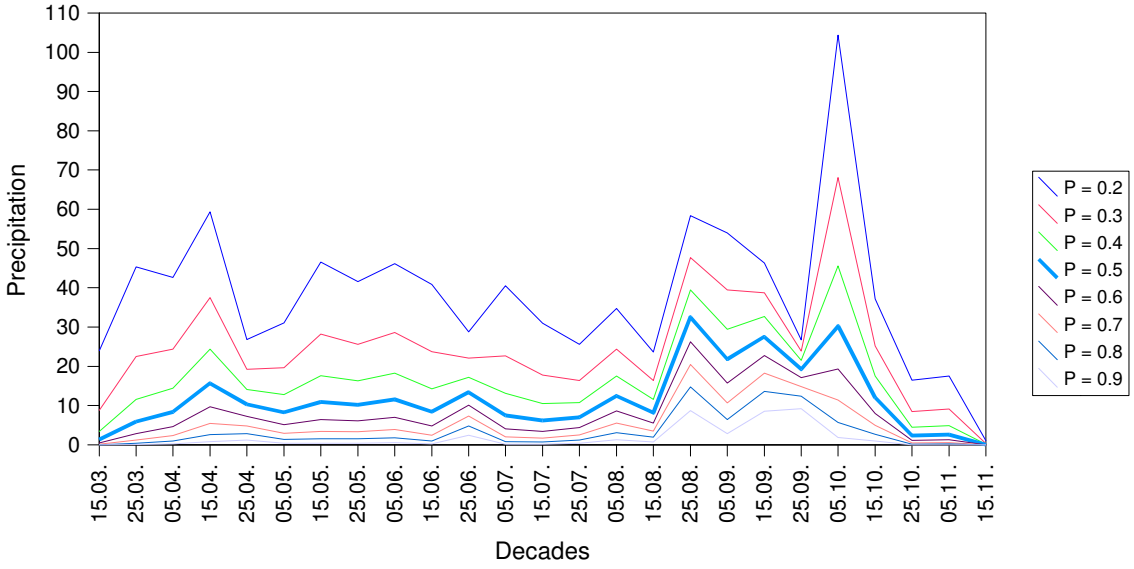

Figure 6.15 Preciptation depths and their probability over the period March – November

The precipitation probability is calculated by equation (3.7). The result for the 8th until the 32th decade is displayed in figure 6.15. For different probabilities (0.2 – 0.9) the corresponding precipitation is drawn at the y-axis. The general pattern in figure 6.15 shows that rainfall increases at all probability levels in both rainy season. Furthermore, a significant low occur in both seasons (April 25th; Sept. 25th).[59] These lows, especially the one in the first rainy season, are surprising. It occurs in the 3rd – 4th decade of April, a period which belongs to the core of the first rainy season. Remarkable are the decades June 25th. (and Sept. 25th). While the rainfall for high probabilities (0.9 – 0.5) have a peak , the

59 In the 2nd season it occures in the suspected flawed decade.

lower probabilities (0.3 – 0.2) hit a low in the same decade. This leads to the conclusion that rainfall occurs always in noticeable sums, but higher precipitation sums (>30 mm) are rare. The opposite case can be observed in the 1st decade of October. High probabilities (0.9 – 0.8) have hit an low, but the low probabilities(0.4 – 0.2) have an extreme peak. Hence, the reliability of rainfall is very low but in the case of rain, it falls in considerable amount. This is also reflected by the high standard deviation for this decade (see figure 6.12).

The diagram depicts that for high probabilities (> 0.5) the amount of rainfall remains small (approx. < 10 mm/decade) for a large proportion of the season. Only a small peak in April occurs. But from mid-August until mid-October the rainfall for a given probability increases in quantity. Interesting is the behaviour of the decades Sept. 25th – Oct. 5th: A sharp break followed by and extremely high peak. This indicates substantial changes between adjacent decades.

6.1.5 Climatic Water Availability for the Reference Crop Sorghum and Terrace Design

The combination of the cumulative precipitation for a specified probability as "supply-function" and the cumulative crop evapotranspiration for the prevailing crop, sorghum, under the local climatic conditions as "demand-function" gives the opportunity to detect water scarcity. The overlay of the two resulting graphs describes the water surplus or deficit over the given growing period. Furthermore, it is possible to estimate the amplifying effect of water harvesting by introducing a water harvesting factor that enhances the precipitation. With simple changes in the rainfall probability and the water harvesting factor, scenarios can be derived to assess the optimal water supply under the given local conditions.

The appraisal of the water demand given by the crop reference evapotranspiration in chapter 3.3 can be combined with a given rainfall depth to access temporal water availability. The given rainfall depth can be derived from the calculations of the precipitation exceedance probability of the Ta'izz data (compare chapter 6.1.4).

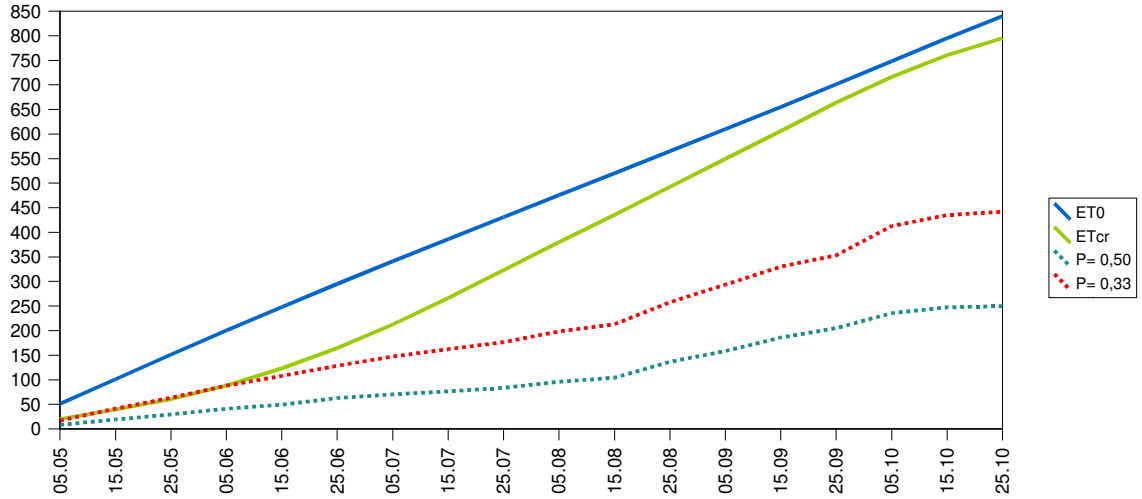

Figure 6.16 Cumulative crop evapotranspiration (ET_{cr}) and precipitation of two probabilities (0.33, 0.5)

With this model it is possible to derive a probability of temporal water availability. Figure 6.16 displays the cumulative functions of reference evapotranspiration (ET_0), crop evapotranspiration (ET_{cr}), and two probabilities of precipitation (0.5 equals a return period of 2 years; 0.33 equals a return period of 3 years). [60]

Figure 6.16 shows clearly the huge gap rising between the crop evaporation for the sorghum reference crop and precipitation. While from Mai until mid-June the gap remains small, it rises to 500 mm (prob. = 0.5) or 300 mm (prob. 0.33) at the end of the vegetation period. This calculation is a conservative risk assessment but it clearly addresses the demand of supplementary irrigation whether it will be provided by ground water or water harvesting. Within this study only the water harvesting case is addressed. Figures 6.17 to 6.19 depict different cases of rainfall probability (0.5 and 0.7), water harvesting factors compared with the reference (ET_0), and crop (ET_{cr}) evapotranspiration. The rainfall probability of 0.5 in figure 6.17 meets a return interval of 2 years. The dotted blue line

60 The parametrisation of crop evaporation for decades is given by the following table:

Stage	***Comment***	***k_c-value (adopted from ALLEN, 1998)***	***k_c-value adapted to local conditions***
Initial kc-ini		0.3	0.39
Development kc-dev	linear rise to	1.1	-
Mid-Season kc-mid		1.1	1.175
Late season kc-end	linear decrease to	0.55	0.74

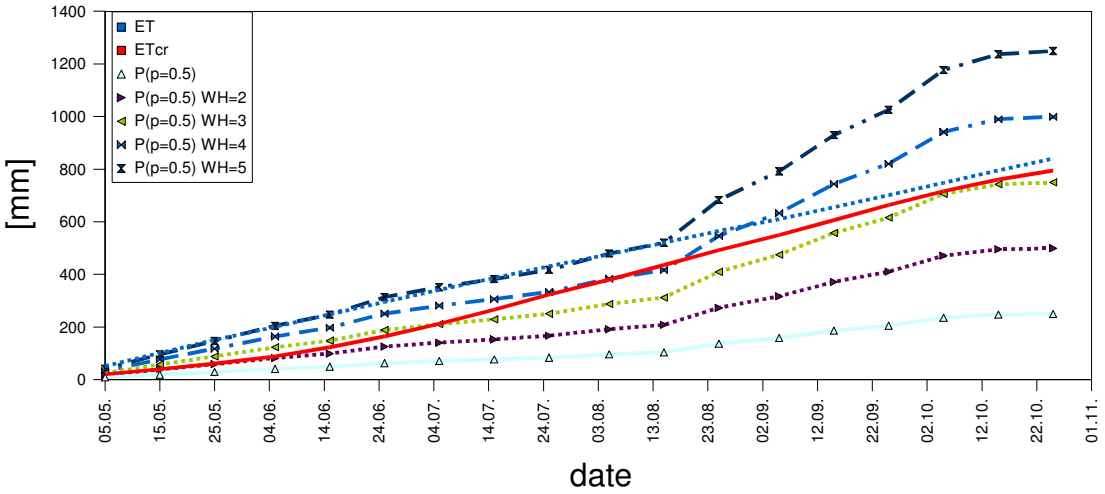

Figure 6.17 Cumulative ET, ETcr and precipitation with a probability of 0.5 and water harvesting factors 2 – 5

represents ET_0 and the solid red line ET_{cr}. Without water harvesting the gap between the water requirements and the supply is dramatic. At any time except at the beginning precipitation will met ET_{cr}.

Only a water harvesting factor of 2 – 3 enhances the rain water supply to a sufficient level. In the beginning and the end of the growing season a factor of 2 is sufficient while in the intermediate dry season a water harvesting factor of 4 is necessary. This estimation of ET_{cr} does not take into account the water saving effects of managing schemes like leaf picking.

A return interval of 2 years does not provide a high reliability for agricultural conditions. Therefore, the probability was increased to 0.7 (return interval: better than 2 out of 3 years) in figure 6.18. Without water harvesting the water availability still remains to low for agricultural purposes. A significant amount of supplementary irrigation provided by water harvesting is needed to meet the agricultural water demand. While during the initial growing phase a water harvesting factor of 4 covers the water requirements, the balance changes at the end of June. The crop evapotranspiration increases noticeably while the precipitation rises only moderately. Hence, the water harvesting factor that covers the water requirements increases considerably. From the end of July until mid-August a water harvesting factor of more than 7 is necessary. From the end of August the precipitation increases substantially. It results in a water harvesting factor of 6 at the end of the growing season.

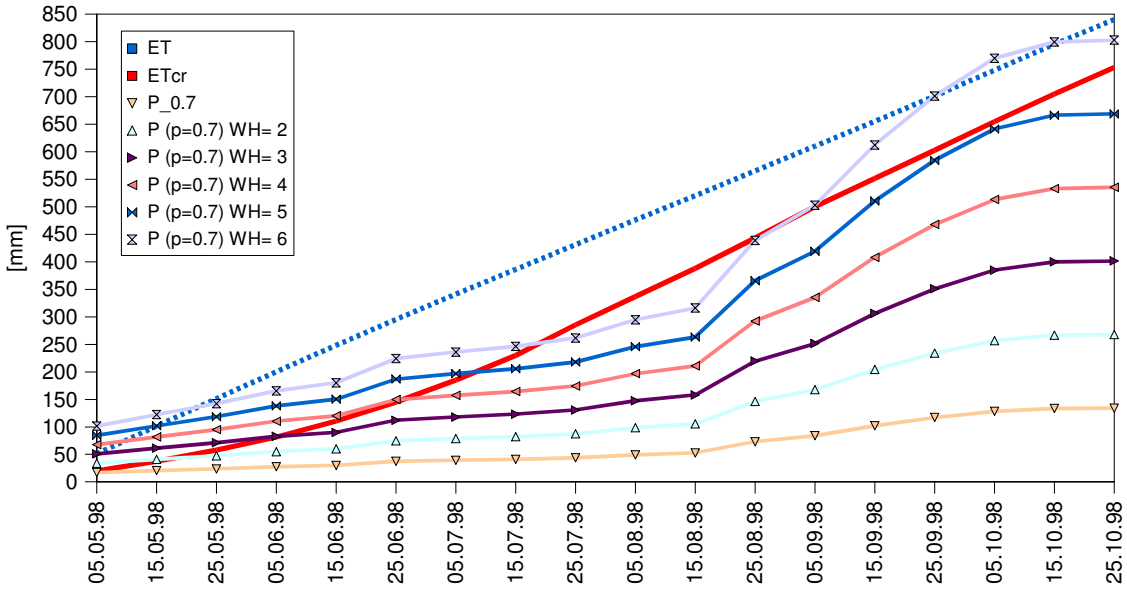

Figure 6.18 Cumulative ET, ETcr and precipitation with a probability of 0.7 and water harvesting factors 2 – 6

This calculation represents the climatic conditions of the Ta'izz area. In the plain areas north of Ta'izz (approx. 1100 m a.s.l.) water harvesting schemes have a relation of water harvesting area to terrace area of 4:1 to 6:1.[61] This calculation seems justified on principle, but not adequate for the Mia'amirah catchment which receives significantly more rainfall.

Therefore, an adjustment to the precipitation is justified. From the short overlapping period of the data sets of Ta'izz and Mia'amirah a factor can only be derived with caution.[62] Nevertheless, an estimation was made to adapt the precipitation depths (factor 2). No correction was done at the evapotranspiration data. The resulte are shown in figure 6.19. For most of the growing season a water harvesting factor of 3 is enough to ensure growing conditions on a probability level of 0.7. In the initial phase a factor of 2 already provides a surplus of water. From mid-July until the beginning of September figure 6.19 shows a water deficit period, the precipitation (with WH = 3) drops below ET_{cr}. At the end of the growing season precipitation exeeds ET_{cr}.

61 Abdulla Aleem, personal communication 1997
62 See analysis of Mia'amirah precipitation data in the following chapter.

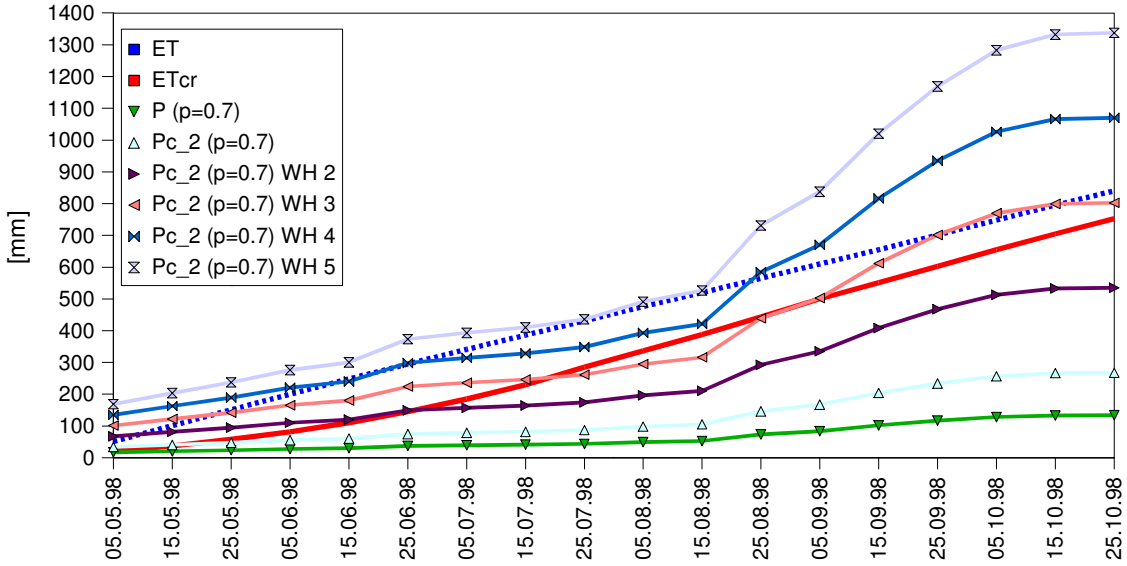

Figure 6.19 Cumulative ET, ETcr and modified precipitation with a probability of 0.7 and water harvesting factors 2-5

6.2 Analysis of the Mia'amirah Data

The climatic analysis focuses on the goal to access the plant available water budget and the efficiency of the water harvesting schemes at catchment scale. Furthermore, a double mass analysis with the Ta'izz precipitation data reveals the relation between the two data sets.

The basic statistics is calculated for all parameters of the meteorological station for the period from 1st March 1998 until 24th Oct. 1998. Only the device for water content in 40 cm depths broke down and is not included. An overview is presented in table 6.6 and figures 6.20.

The course of precipitation (*P*) in figure 6.20 shows a little precipitation in the beginning of March while the first significant rain starts in the 2nd decade of May. But the precipitation in the first rainy season remains infrequent. On the contrary, the second season has high and frequent rainfall that sharply diminishes after 9th Sept.1998. As expected, the relative humidity (*RH*) respond directly to rainfall events. Inversely, the radiation decreases due to the cloud cover. The daily temperatures range in a relatively small interval between 15°C and 26°C without a significant seasonal development.

Table 6.6 Basic statistical parameters of the meteorological station

	RH [%]	Tair [° C]	IRR_d [W/m²]	Tsoil 80 [° C]	Tsoil 60 [° C]	Tsoil 40 [° C]	wind spd [m/s]	Water content soil 80 cm [%]	Water cont. soil 60 cm [%]	Pair [mb]	Precip [mm]	ET_0[63] [mm]
mean	59.28	21.74	256.67	24.61	24.70	24.82	1.73	0.31	0.31	817.62	3.89	4.64
median	59.51	21.58	263.58	24.80	24.90	24.86	1.71	0.28	0.31	817.60	0.00	4.38
stdev	16.57	2.22	54.07	1.89	1.98	2.23	0.39	0.12	0.11	1.87	8.79	1.87
skew	0.19	-0.16	-1.22	-0.15	-0.13	-0.06	0.83	0.35	0.15	0.04	3.20	0.13
kurtiosis	-0.36	-0.03	2.15	-0.37	-0.31	-0.42	1.32	-1.50	-1.63	-1.04	11.24	-0.30
min	21.53	15.43	48.92	19.82	19.53	18.97	1.01	0.17	0.18	813.63	0.00	0.23
max	99.99	26.30	336.77	28.43	28.89	29.78	3.35	0.53	0.48	821.35	53.75	8.95

Figure 6.21 depicts the volumetric water content (WC) at 60 cm and 80 cm depth, temperature at 40 cm, 60 cm, 80 cm and precipitation. During the dry season WC levels off at 18 %, near the permanent wilting point (PWP). The first significant rain (12 mm on 5th May) does not have any effect on the water content in that depth. Only after the amount of 73 mm within 3 days (May 12 – 14) the WC jumps from 18 % to 45 %, from where it decreases linearly interrupted by some signal from the major rainfall events to approximately 23 % from where is levels out until it increases rapidly to 37 % (Aug. 8). From this level it increases again and responds to every daily rainfall larger than 15 mm.

It was first assumed that during the first period the field did not receive additional runon irrigation while in the second phase the inlets were opened and the terrace receives more water. But alternatively another interpretation is possible: The sensors are relatively deep. The terrace has a sandy loam texture with a total pore space of 47 % and an available moisture content (AMC) of about 90 mm/m or more.[64] Approximately 50 mm of water can be stored in the soil column above the sensors. Furthermore, the soil conductivity reduces with dryness. Therefore, under dry conditions (as in the first rainy season) smaller rainfall events may not reach the sensors, but a similar event under wetter conditions (as in the second rainy season) would have an impact.

63 ET_0 is calculated by equation (3.9)

64 The texture analysis in the laboratory ascertain "sandy loam" while the field values of total pore space may indicate finer texture (loam).

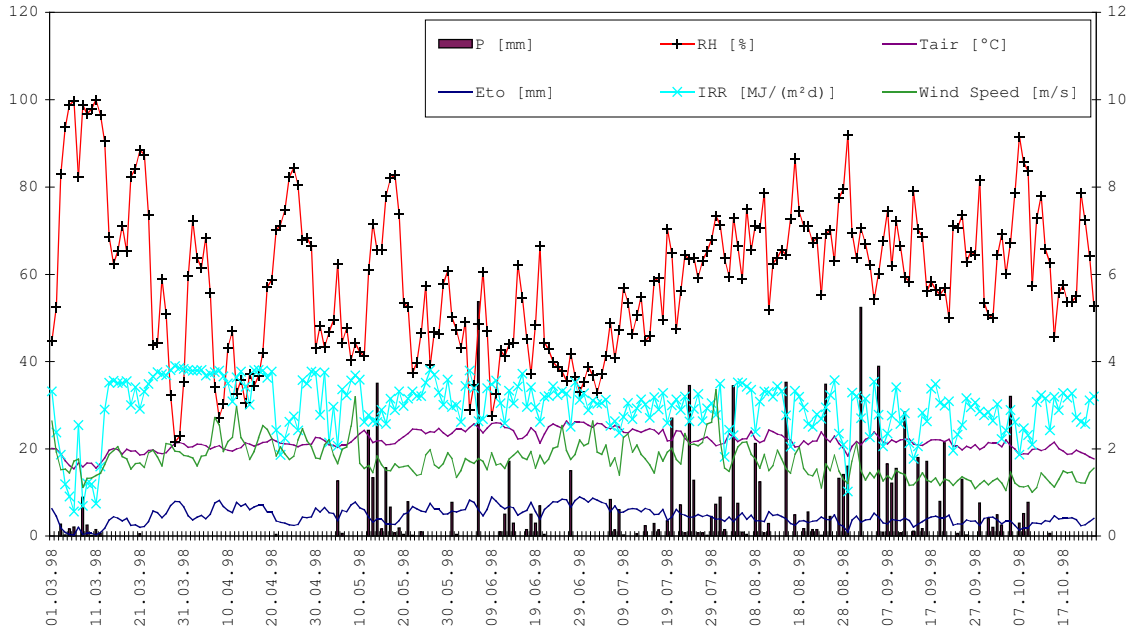

Figure 6.20 Daily meteorological observations of the weather station Mia'amirah

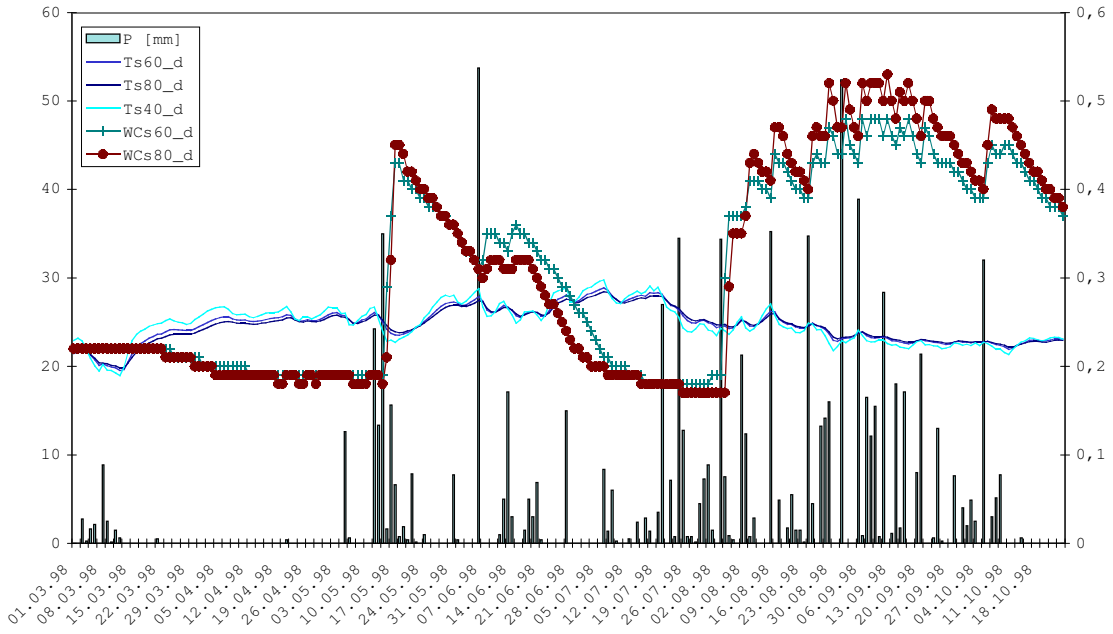

Figure 6.21 Daily precipitation, soil temperature and soil water content

6.2.1 Precipitation

Precipitation is analysed with regard the typs of rainfall, how it supplies for the plants and how it triggers runoff. The rainfall frequency fits the exponential distribution (figure 6.22), but has a peak in the class of 30 – 35 mm which cannot be represented by the theoretical model.[65] This local peak indicates that there is a considerable number of large rainfall events that are able to produce runoff. Figure 6.23 reinforces this assumtion. In this figure the count of each class is multiplied with the class centre and divided by the total amount of precipitation of the measurement period. It represents the percentage of the total rainfall volume of each class. The graph of the probability density function declines from 15 % for the 0 – 5 mm class down to 6 % for the 25 – 30 mm class. Only the 15 – 20 mm class produces a local peak. The 30 – 35 mm class rises dramatically to 17 %. For higher rainfall classes it varies: 5 %, 0 %, 0 %, 11 %. 36 % of the total rain falls in events larger than 30 mm. Such strong events definitely produce runoff in no-terrace zones.

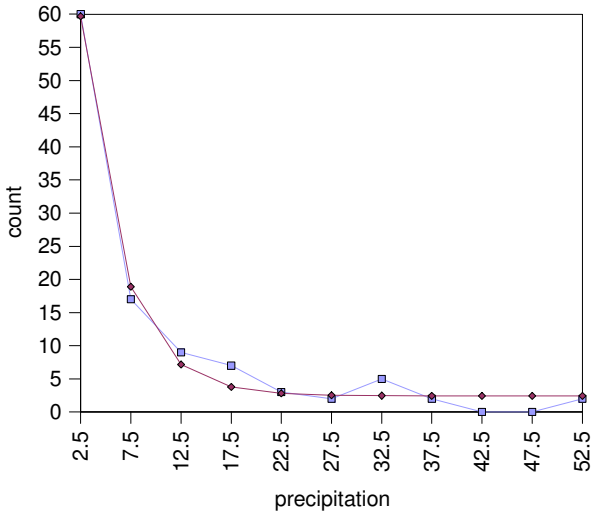

Figure 6.22 Frequency distribution of Mia'amirah daily precipitation and exponential fit

The Ta'izz precipitation data are used for long term considerations since it is the nearest meteorological station with long term record. The straight distance between both stations is approximately

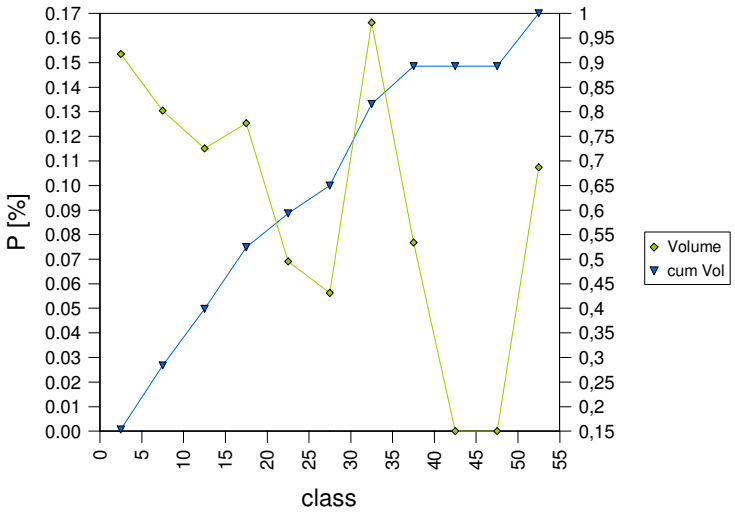

Figure 6.23 Percentage of daily precipitation by class as density and cumulative function

65 Wilcoxon Rank-Sum test: (p= 0.29 > than the significance level $\alpha = 0.05$) result: the distribution of daily rainfall can be approximated by an exponential model.

40 km, which is considerable for such a mountainous area. The difference in altitude comes to 600 m. In such circumstances, differences between the stations are probable and must be accepted. Nevertheless, the correlation between the stations should be verified.

Rain in the Southern Uplands is mostly triggered by convective weather conditions. These convective cells have only limited extent.[66] Hence it can be assumed that precipitation events in Ta'izz and Mia'amirah are not induced by the same cell. Accordingly, no correlation between the daily data can be expected. But due to climatic similarity of the region the decade sums should correlate. The double mass analysis is used to test the dependency between the two data sets. The double mass plot in figure 6.24 shows the decade precipitation of the period March – October. It describes reasonably good agreement between the two stations. Most obvious is the significantly higher amount of precipitation indicated by the gradient of the regression line of 0.5. During this limited period, Mia'amirah receives almost twice as much as Ta'izz. This has to be concerned in the results of the exceedance probability that are used for Mia'amirah.

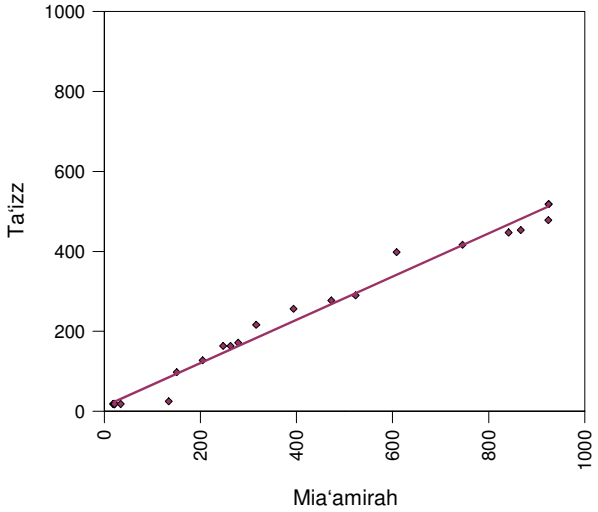

Figure 6.24 Double mass plot: Mia'amirah and Ta'izz decade precipitation, overlapping period: Jan. – Oct. 1998

66 WRAY-35 (1995): 10 – 15 km diameter

6.2.2 Selected Precipitation-Runoff Events

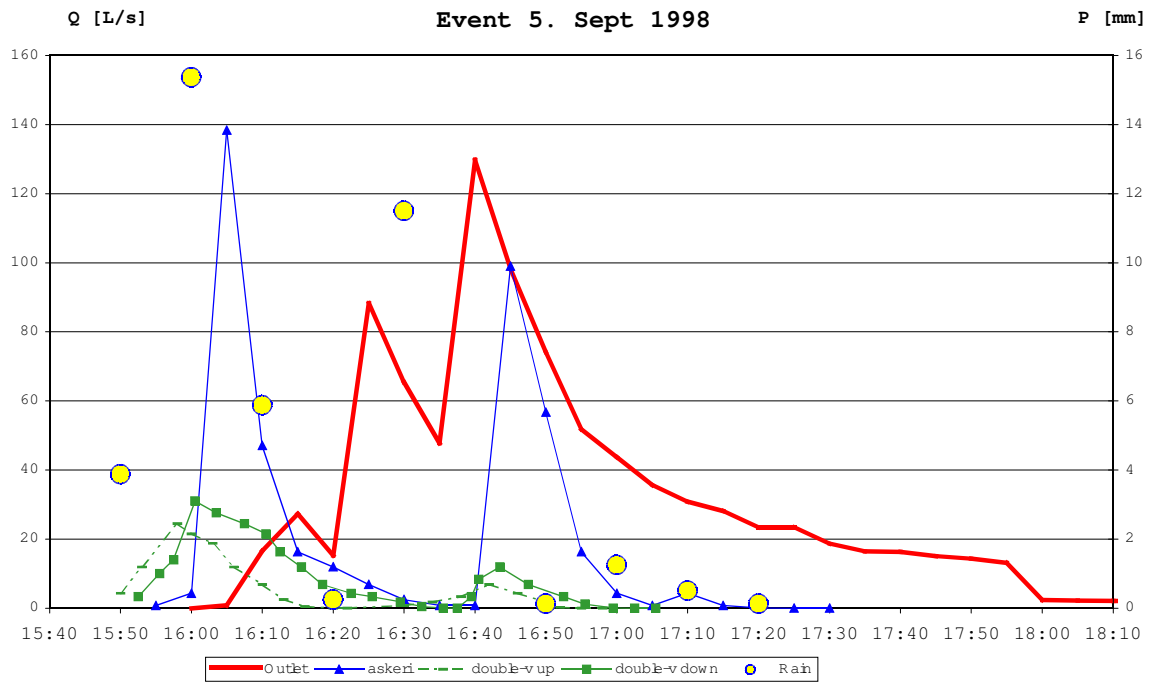

Figure 6.25 Runoff hydrograph of 9th Sept 1998

During the measurement period in 1998 10 events could be measured in all locations. The resulting hydrographs are given in appendix 9.4. Selected hydrographs are shown in figure 6.25 and figure 6.26. They show the rainfall runoff events of the 5th Sept. 1998 and 9th Sept. 1998. The event on 5th Sept. 1998 was with a total sum of 38.9 mm precipitation the strongest of all measured events in 1998. Rainfall started at 15:50 h and continued until 17:20 h. The temporal distribution has a double peak with high intensities (16:00 h, 92/mm/h; 16:30, 69 mm/h) which is reflected by the hydrographs of all outlets. The shape appears as a typical shapes of triangle “flush-flood” form. Most distinguished is the gauge “askeri” which also reaches the highest peak discharge (138 l/s), while the main outlet reaches only 130 l/s. Further, also the main outlet has a typical peak flow hydrograph but a very small tailing (approx. 1 l/s) that remains beyond midnight. It is assumed that it came from intermediate storage. The double-v gauge contributed with a peak flow of 31 l/s and 24 l/s respectively.

The rainfall event on 9th Sept. 1998 has a total of 15.5 mm. That is half of the amount of the 5th Sept. 1998 event. The precipitation distribution is unimodal and 75% of the total rainfall fell within 10 min. The runoff response at the main outlet is with a peak discharge of 234 l/s almost twice as much as at the event on 5th Sept. 1998. The peak flow at the gauge "askeri" is with 88 l/s 40% smaller as the during the preceding event. The peak discharge at the double-v gauge contributes with 99 l/s and 121 l/s.

The main difference in the response of the 2 precipitation events is caused by the precipitation of the 4 preceding days. The amount of rain before the 9.Sept. 1998 event was 68 mm, while the 4 days before 5th Sept. 1998 received no rainfall.[67]

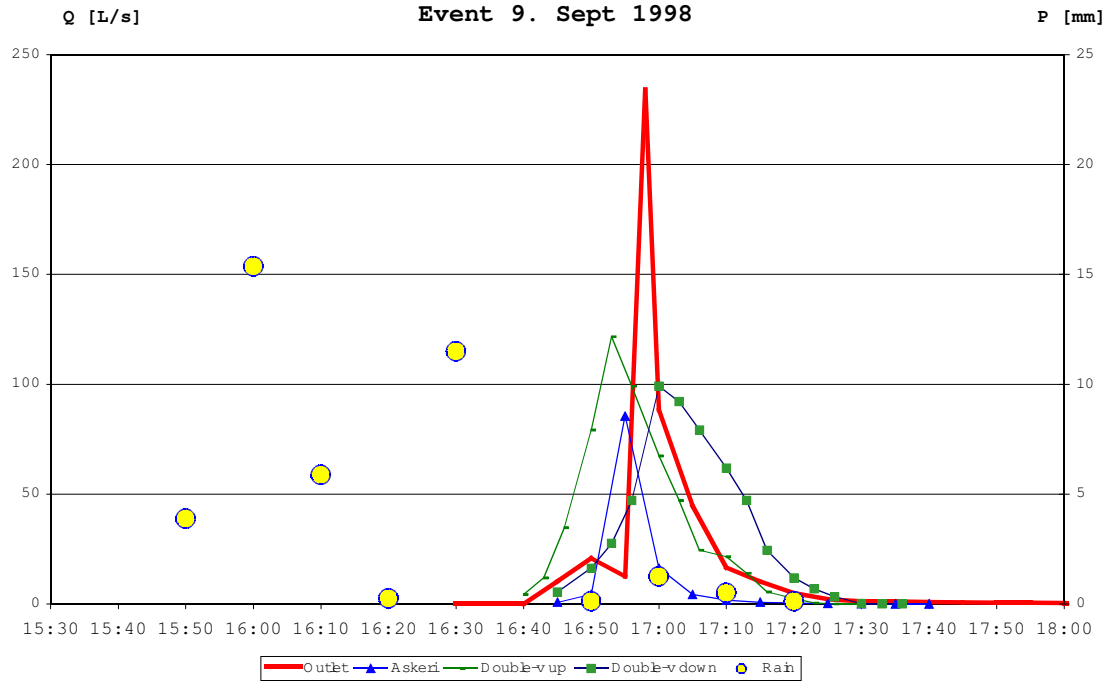

Figure 6.26 Runoff hydrograph of 5. Sept 1998

6.2.3 Infiltration

Figure 6.27 displays the results of the infiltration experiments. The x-axis represents the time from the start of the experiment, the y-axis the infiltration rate. The experiments divide into two categories: High infiltration rates for the sites "grove" and T 528. Both are located almost in the center of the valley. The terrace T 528 has clay loam. The rate starts at the very high level of 50 cm/h and decreases smoothly to 25 cm/h. In contrast the experiment at "grove" shows an irregular pattern. The infiltration rate starts with 40 cm/h,

67 However the preceding rainfall on 1st Sept. 1998 was with 52 mm the 2nd biggest event in the period of measurement.

drops to 32 cm/h and increases sharply to 47 cm/h. With some alternating it reduces to 30 cm/h after 2:30 h. Then it rises again. Presumably, at this location with wood, marcopores are more prevailing. Also T 327 is a fallow terrace. The infiltration is low and the soil appears compacted, enforced by goat and cattle grazing. The infiltration rate at terrace T 431 is surprisingly low, although the texture is clay loam.

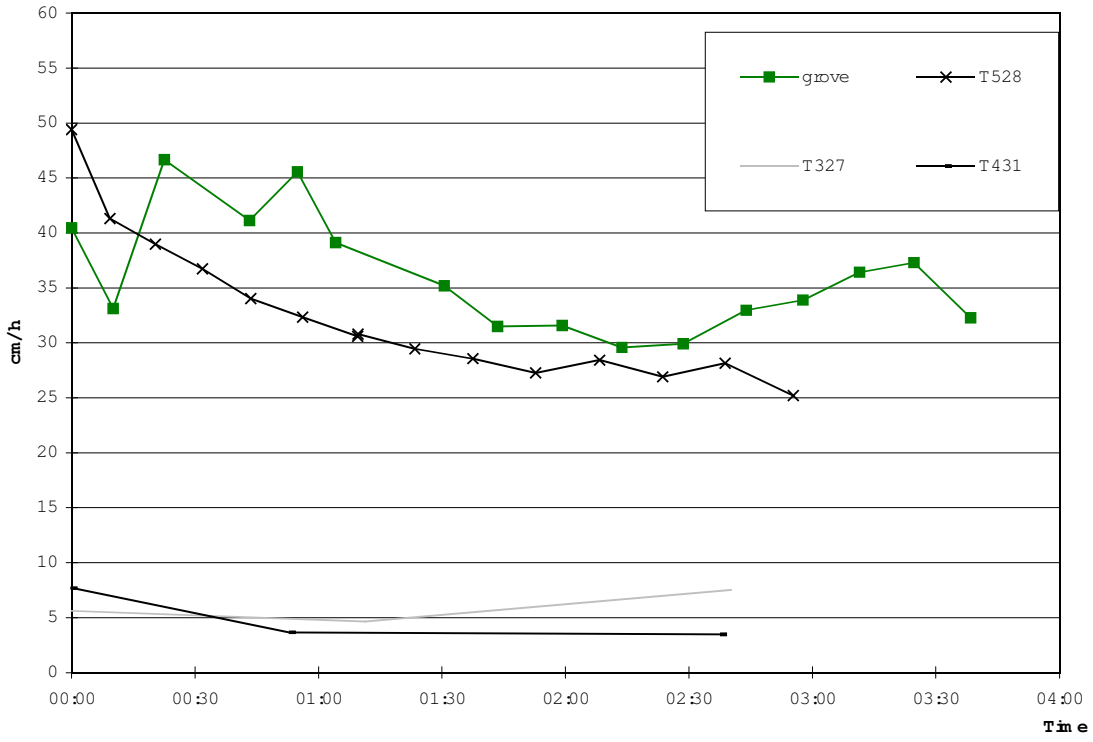

Figure 6.27 Infiltration plots

6.3 The Crop Evapotranspiration Model with and without Water Harvesting Component

The crop evapotranspiration model with and without water harvesting component compares two model-scenarios to derive the efficiency of the existing water harvesting schemes under the given rainfall of the 1998 rainy season. In the scenario without water harvesting it was assumed that no water harvesting effect existed and that there were only pure rainfed conditions. The second scenario runs with the same parametrisation but includes the effect of water harvesting. The model is based on the concept of crop evapotranspiration explained in chapter 3.3. The advantage of modelling the depletion of the soil body by evapotranspiration is that a 1-D approach can be used because

evapotranspiration is always vertically oriented. This approach is extended to a semi-distributed model. The spatial variability is considered by a classification of the terraces into homogeneous zones. The model is applied to each zone. The zones were assigned with different parameter sets. Water harvesting is incorporated as water harvesting factor (see chapter 3.1.1). The model computes the daily dual crop coefficient and multiplies it with the reference evapotranspiration to calculate the actual depletion. The readily available water, *RAW,* and the total available water, *TAW,* are calculated as benchmarks for water stress and permanent wilting conditions. The main goal of the model is to investigate the temporal and spatial water availability under different water harvesting and management conditions.

6.3.1 Parametrisation of the Model

For the correct calculation of the depletion the model requires detailed information about the reference crop, the climatic conditions and the soil. Since the model is not a vegetation growth model, information about the plant development is also required as input data.

The length of growing stages was selected from DOORENBROS and PRUITT (1977) and referenced in the field by own observations and consulting of local farmers. In agreement with the local farmers the season was considered from May until the the end of October. This period of approximately 180 days for the reference crop sorghum is considerably longer than indicated in the literature (e. g. 130 -140 days, DOORENBROS and PRUITT (1977), ALLEN et al. 1998). Especially the crop development stage and the mid-season stage are with 55 days and 70 days respectively significantly longer. The length of the stages is given in table 6.7.

The basal crop coefficient k_{cb} for all growing stages is taken from ALLEN et al. (1998). The initial rooting depth depends on how deep the seeds are set into the soil. A planting stick is usually used for sowing, therefore an initial rooting depth of 20 cm is assumed. The maximum rooting depth for sorghum is estimated at 1.75 m if the terrace depth was sufficient. Otherwise the terrace depth is taken as maximum rooting depth. The maximum plant height under good growing condition was measured in the field with 2.5 m. The

readily available water (*RAW*) is estimated at 70 % of the total available water (*TAW*) in the initial stage and at 50 % after the initial stage. These lumped parameters are listed in table 6.8.

Table 6.7 Lengths of crop development stages for grain sorghum in Mia'amirah

Stage	***Start***	***Day of Season***	***Duration (local)***	***Duration (literature)***
Initial	1st May	1	25	20
Development	26th May	26	55	35
Mid-Season	20th July	81	70	45
Late season	28th Sept.	136	30	30
End of meteorologic measurements	24th Oct.			
End of season	31st Oct.	180	180	130

Table 6.8 Overview of the standard model parameters, values derived from ALLEN et al. (1998)

Parameter	***Unit***	***Description***	***Value***
$K_{cb\ ini}$	[1]	Basal crop coefficient initial stage	0,15
$K_{cb\ mid}$	[1]	Basal crop coefficient mid-stage	1,05
$K_{cb\ end}$	[1]	Basal crop coefficient final stage	0,9
Max height	[m]	Maximum plant height	2,5
RAW during initial stage	[%]	Readily available water (*RAW*) in percent of total available water (*TAW*) during initial stage	0,7
RAW after initial stage	[%]	Readily available water (*RAW*) in percent of total available water (*TAW*) during initial stage	0,5
initial D_e	[mm]	initial moisture content in the top soil	20

For the representation of spatial variability homogeneous zones were classified on the basis of the terrace depth and the available water content (*AWC*) of the soil. For the terrace depth 3 groups, (< 1 m, 1 – 1.5 m, > 1.5 m) are used. The available water content was derived from texture class (figure 4.6). It was categorised into poor (66 mm/m), moderate (110 mm/m), good (180 mm/m) and excellent (215 mm/m). The resulting matrix is given in table , the classes are marked with single letters from '*a*' to '*j*'.

Figure 6.28 shows the map with the spatial pattern of these classes. The classes *a,b,c* represent terraces with low storage capacity, they occur in top slope areas. Class *a* only occurs in small and steep uphill locations in the south eastern part while class *b* has its major extent in the steep up-slope area in the south western part of the catchment. Class *c* occurs in two locations at the western up-slope.

Table 6.9 Model classes with applied water harvesting factors

Class	***Water Harvesting Factors Applied***
a	2.5
b	1.5, 2.5, 3.5
c	2.5
d	1.5
e	1, 1.5, 3.5
f	1, 1.5, 2.5
g	1, 1.5, 2.5
h	1, 1.5
i	1
j	1, 1.5

Table 6.10 Matrix of different combinations of terrace depth and available water content (AWC)

	Terrace depth [m]		
AWC [mm/m]	***0,75***	***1,25***	***1,75***
66 (poor)	*a*	*b*	*c*
110 (moderate)		*d*	
180 (good)	*e*	*f*	*g*
215 (excellent)	*h*	*i*	*j*

The steep up-slope locations in the volcanic south western part of the catchment are almost completely occupied by class *b*. Class *a* only occurs in small and steep uphill locations in the south eastern part and class *c* occurs in three uphill locations at the slopes in the west and south. These classes represent terraces with poor available water content, *AWC*. Underneath the slope is predominately classified by *f*, the most prevailing class of the catchment. It also covers the lower parts of the catchment and the steeper areas of the in general more gentle eastern slopes. The remaining, more levelled slopes are mostly occupied by class *e. C*lass *g* is embedded in class *f* and has only limited extent. These three classes have the same *AWC*-class but differ in the terrace depth. Class *d* covers only a small area near the main runoff channel, it has the same terrace depth as the surrounding terraces but a lower *AWC*. Class *i* occurs at a relatively gentle middle slope in the western part of the catchment. It has the same terrace depth as the surrounding class *f* but a better *AWC*. Embedded is a little area of class *j*, which has a bigger depth. The class *h* covers a slightly sloped area above the graveyard. It is shallow but has an excellent *AWC*. The spatial extension of the zones is merged with the spatial extension of the different water factors showed in figure 5.3. The result is a

combination of terrace zone and water harvesting factor. This increases the number of zones to 20. They are given in table . The overview of the spatial distribution is given in figure 6.28.

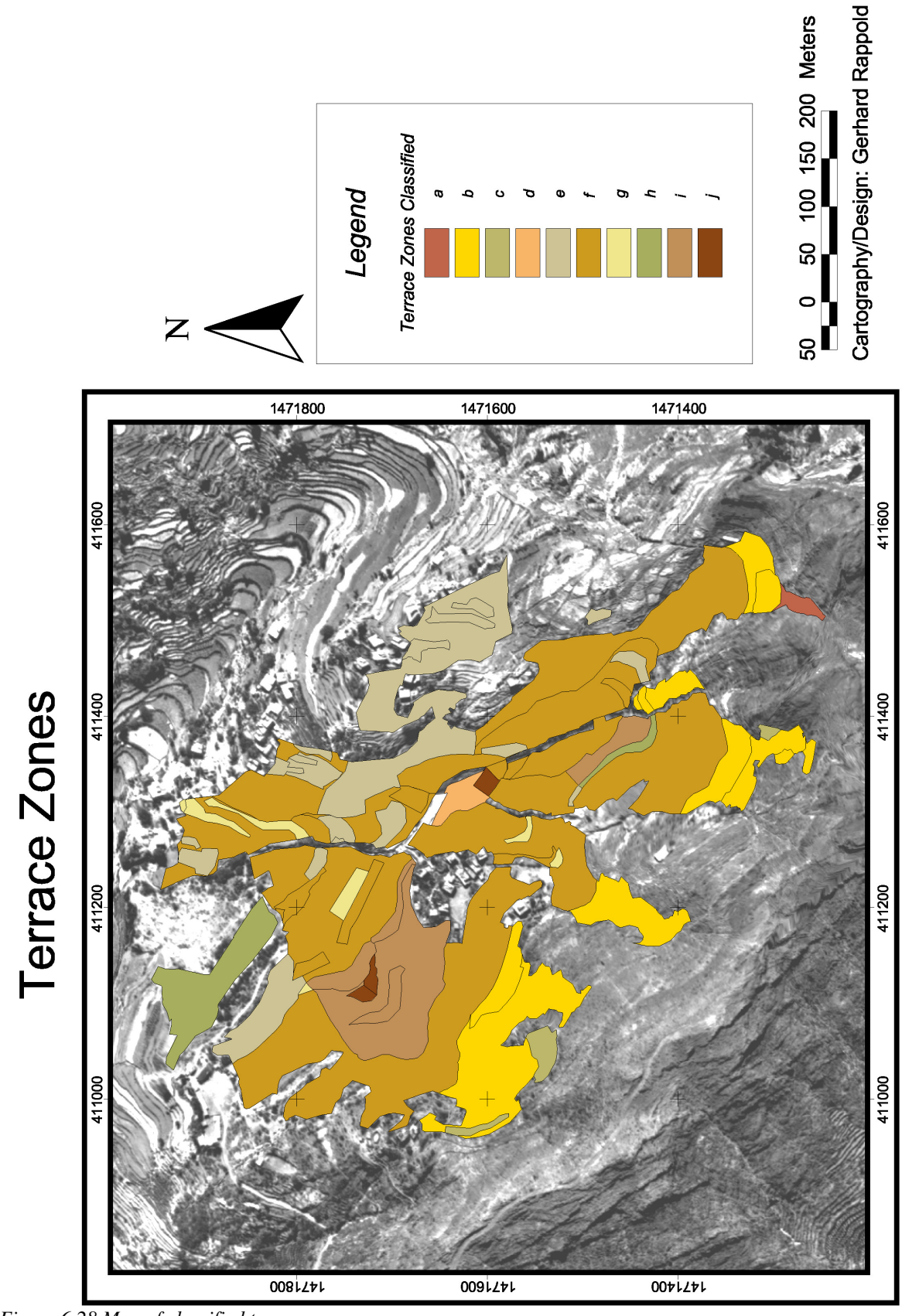

Figure 6.28 Map of classified terrace zones

6.3.2 Model Results

The model results are displayed in figure 6.30a–j by two diagrams for each zone. The different scenarios are given by the different graphs in the diagrams. The upper diagram shows the change of the basal crop coefficient (k_{cb}) and the dual crop coefficient $k_{cb} \cdot k_s + k_e$ for each water harvesting factor, all dimensionless in the 1st y-axis and precipitation in millimeters in the 2nd y-axis. The lower diagram depicts the depletion in millimeters. Each water harvesting factor is represented by its own graph. The y-axis is in reverse order to make it more obvious that the depletion results in a reduction of soil moisture. The diagrams show the depletion from the soil body and its recharge by rain. Zero indicates saturated conditions at field capacity. Water supply for the plants is optimal if the actual depletion ranges between zero and *RAW*-level. Below *RAW* water stress occurs and the *TAW*-benchmark indicates the permanent wilting point. Since the model is not a plant growth model but an evapotranspiration model, no abort conditions stop the calculation at the permanent wilting point (*PWP*). Since the goal of the modelling is to evaluate the water harvesting effect over the full period, such behaviour is desired.

6.3.2.1 Rainfed Scenario

The rainfed scenario is given by the "*act. depl. rainfed*" graph in the diagram of each zone. All zones (figure 6.30a–j) show a general pattern for the course of the crop coefficients and the depletion and restocking by rain, but with significant differences. During the initial and the development stage rainfall events are sparse compared to the frequent rain during the mid and late season stages. In the initial stage the similarity of the graphs between the different zones is high. This is caused by the limited rooting depth which keeps the variation between the classes small. Especially the classes which are only separated by the terrace depth do not show any difference because the total storage capacity is limited by the rooting depth and not by the terrace depth (*a, b, c* ; *e, f, g* and *h, i, j*). The graphs of the dual crop coefficient $(k_{cb} \cdot k_s + k_e)$ show major changes in all zoned during the initial stage. This dynamics is caused by the significant influence of the evaporation

component k_e which raises to 1.15 and increases the evapotranspiration to its maximum. Moreover, the thin soil layer also recharges quickly by rain. These two effects cause a high dynamic response to depletion and recharge.

The diagrams in figure 6.30*a–c* show terraces with a low *AWC* (compare table) that results in low *TAW*-volumes. At this stage, these zones in some cases exceed the *TAW*-limit. This is also a consequence of the strong influence of the evaporation component k_e in the upper soil layer. If the rooting depth is equal to the depth influenced by evaporation (0.2 m) the evaporation forces are able to lower the depletion below the permanent wilting point (compare equation 3.15). This causes the plants to dry up. In this non-calibrated model the model run was not stopped and continued under the given conditions to evaluate the water harvesting effect.

In the development stage the *TAW* rises corresponding to the increase of the rooting depth. The maximum *TAW* is reached at the end of the development stage. The dominant process in all zones during the development stage is the depletion. In all zones the *TAW*-benchmark was exceeded at the end of the initial stage and the development stage started with a period of water stress which was recovered by the major rainfall event of 53 mm on 6th May. In the zones with limited storage capacity (*a*, *b*, *c, e*) the gain lasts only for 2 – 3 days while the zones with large storage capacity (*f, g, i, j*)are released for a longer period (16 – 27 days). Rain recharges in all zones in the same amount. This causes the effect that the zones with limited *AWC* get recharged more rapidly while in the zones with higher *AWC* the same amount of recharge has a smaller effect.

Immediately with the beginning of the mid-season rainfall increases in quantity and frequency. In all zones the recharge dominates depletion. The time until saturated soil conditions are reached depends on the level of depletion in the previous stage and the *AWC* of the particular zone. While zone *a* reaches field capacity for the first time already 24th July and zone *b* 9th August, it takes longer for the other zones. The zones *c, d, e* reach field capacity 28th and 29th August, *h* on 1st September and *f* 5th September. The *RAW*-level which indicates the release from water stress is crossed already in the 2nd half of July. After the field capacity is reached in every zone depletion never exceeds a critical level until the

precipitation stops at the end of the growing season. Then the dry period begins which depletes all soils considerably. At this stage the crop maturation is finished and and water stress does not affect the plant development to a major extent.

6.3.2.2 Water Harvesting Scenario

The water harvesting scenario compares the effect of the different water harvesting factors in the particular zone with the rainfed conditions. The graph are displayed in the same diagrams of figure 6.30a–j.

In the initial stage the differences between the rainfed and water harvesting scenario remain relatively small but perceptible, e. g. the rainfall event on the 5th May shows (good to recognise in zone *b* and *e*) that water harvesting reinforces the recharge process. Surprisingly, in zone *a*, *b,* and *c* the following depletion becomes more severe in the water harvesting scenario than in the rainfed scenario. Nevertheless, after the rainfall on 5th May the course of the graphs in all zones remains still close to the rainfed graphs. The small effect during the initial stage is caused by the limited *AWC* of the considered soil layer. The soil layer is limited by the initial rooting depth of 0.2 m, therefore differences in the terrace depth show now effect and the total *AWC* of this soil layer becomes saturated already by the small rainfall events. The number of days with water stress in the initial stage is shown in figure 6.29a. On the x-axis the different water harvesting factors are shown. The y-axis displays the days with water stress. The length of the y-axis is equivalent to the length of the growing stage. The diagram shows that the number of days with water stress is considerably high in the rainfed scenario in most zones. The reduction by water harvesting is relatively small.

The effect of water harvesting becomes more significant in the development stage. With the increase of the rooting depth in all zones the differences between the rainfed scenario and the water harvesting scenarios rise. The zones with a water harvesting factor of 1.5 remain relatively close to the rainfed scenario in the development stage (zones *b*, *d*, *e*, *f*, *g*, *h*, *i*, *j*). With the factors 2.5 and 3.5, however, the effect increases remarkably.

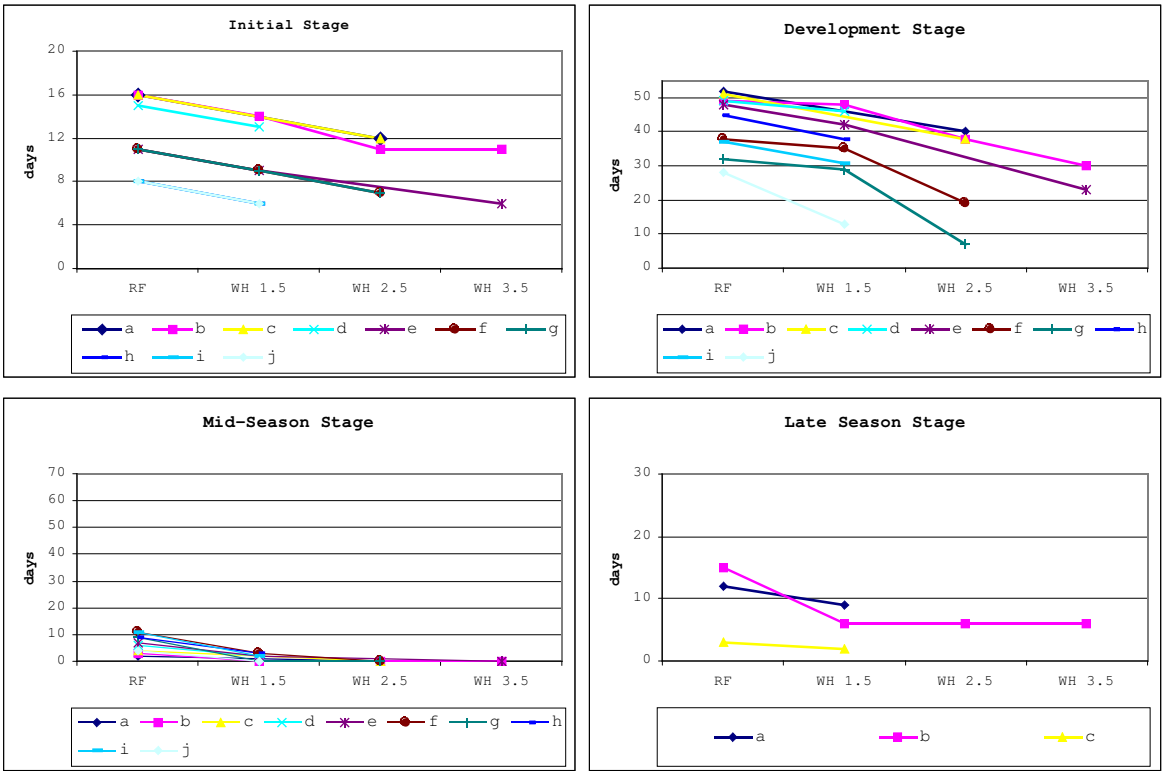

Figure 6.29a-d Days of water stress in the different growing stages

As mentioned before, depletion is the dominant process in the rainfed scenario, while in the water harvesting scenario the relation between depletion and recharge is more dynamical. In the zones *a*, *b*, *c*, *e,* and *f* recharge causes nearly saturated conditions several times in the developing stage.

It is noticeable that in the zones *a, b, c* the depletion rate after rainfall events (events on 6th, 13th, 20th and 27th June) in the water harvesting scenario is higher than in the rainfed scenario. Therefore the depletion level, which is reached before the next rainfall is nearly the same as in the rainfed scenario. That shows that the water reserve in the development stage of these zones gained by water harvesting is usually small and provides additional water supply only for a few days.

In contrast, zones *e–j* the combination of *AWC* and the water harvesting factors of 2.5 and 3.5 lead to an effectiv recharge. The depletion does not reach the same level as the rainfed scenario. For example, in the rainfed scenario in zone *e* the period of water stress (exceeding of the *RAW*-benchmark) starts on 15th June and ends on 24th July. The water harvesting scenario (water harvesting factor 3.5) crosses the *TAW*-benchmark slightly on

26th June for one day, for a 4 days period from 2nd July – 5th July and from 12th until 19th July. The number of days with water stress in the development stage in zone *e* reduces from 48 to 23 (see figure 6.29b). The water harvesting factor of 3.5 delays the water stress for 2 weeks and reduces its magnitude. The effect is similar in the zones *f* and *g* for factor 2.5. The number of days with water stress reduces from 38 to 19 and 32 to 7 days respectively. For the water harvesting factor 1.5 the reducing effect is less strong. Therefore, the reduction effect is not that strongly developed in zone *i* (period of water stress reduces from 37 to 31 days) but surprisingly high in zone *j* (periode of water stress reduces from 28 to 13 days). At the end of the development stage the level of depletion in all zones is high.

By coincidence, in the beginning of the mid-season stage with more frequent rainfall the pattern of depletion and recharge changes. Recharge becomes the prevailing process. Therefore, the period of recharge until saturated conditions in the mid-season stage is used to compare the recharge effect of the different scenarios. Zones *a* and *b* recharge, due to their low total *AWC* in very short time. Zone *a* (factor 2.5) reaches saturated conditions already by the rainfall of 27 mm on the first day of the mid-season stage (20th July). It takes only 3 days more in the rainfed scenario. In zone *b* the water harvesting factors 2.5 and 3.5 also reach saturated conditions with the first rain while it takes two more rainfall events to recharge zone *b* with water harvesting factor 1.5 (24th July). But the rainfed scenario reaches saturation 16 days later on 9th August. In all other zones the difference between rainfed and water harvesting scenario is even bigger. In zones *c, d, e,* and *h* saturated conditions are reached between 28th August and 1st September. The corresponding water harvesting scenarios have much shorter recharge times. The zones *d, e,* and *h* with water harvesting factor 1.5 shorten the period until saturation is reached by 27, 26 and 24 days respectively. For the water harvesting factors 2.5 in zone *c* and 3.5 in zone *e* the reduction is 35 and 40 days.The remaining zones *f*, *g*, *i,* and *j* have a reduction between 21–29 days (water harvesting factor 1.5) and 35–43 days (water harvesting factor 2.5). The comparison between the rainfed and water harvesting scenario shows the efficient reduction of the recharge time from the rather empty soil storage at the end of the development stage until

saturation in the mid-season stage. The figure 6.29c shows that the days of water stress are 11 or less under rainfed conditions. The water harvesting decreases the water stress to 0–3 days.

Shortly after the beginning of the late-season stage on 28th September the rainy season stops on 9th October. In all zones, regardless whether rainfed or water harvesting scenario the course of depletion is linear. All graphs are identical until the *RAW*-level is crossed in the zones *a*, *b,* and *c*. In the diagram of days with water stress (figure 6.29d) only those zones are displayed. The reduction of days with water stress does not depend on the magnitude of the water harvesting factor.

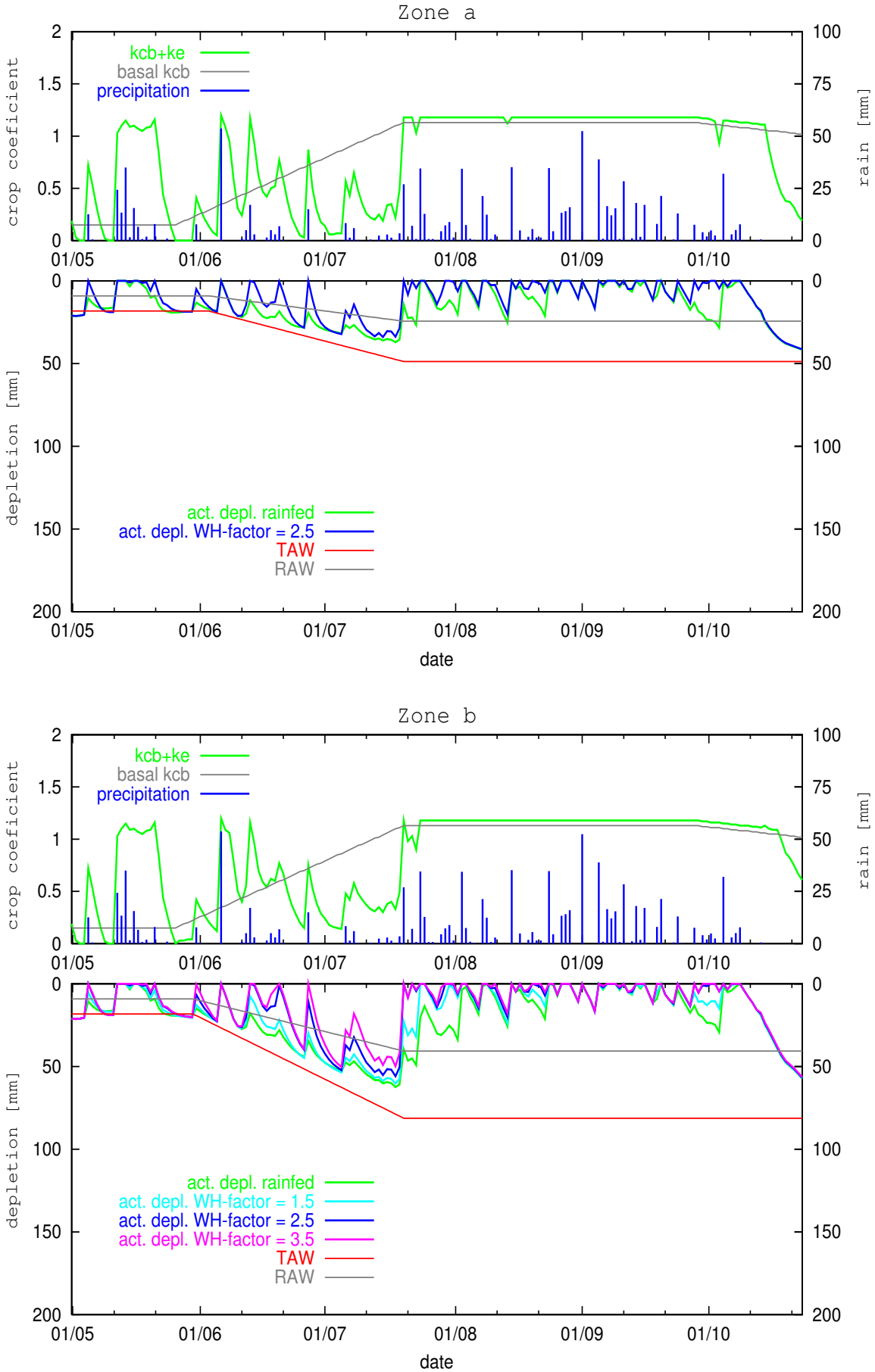

Figure 6.30 Model results of different zones without and with water harvesting

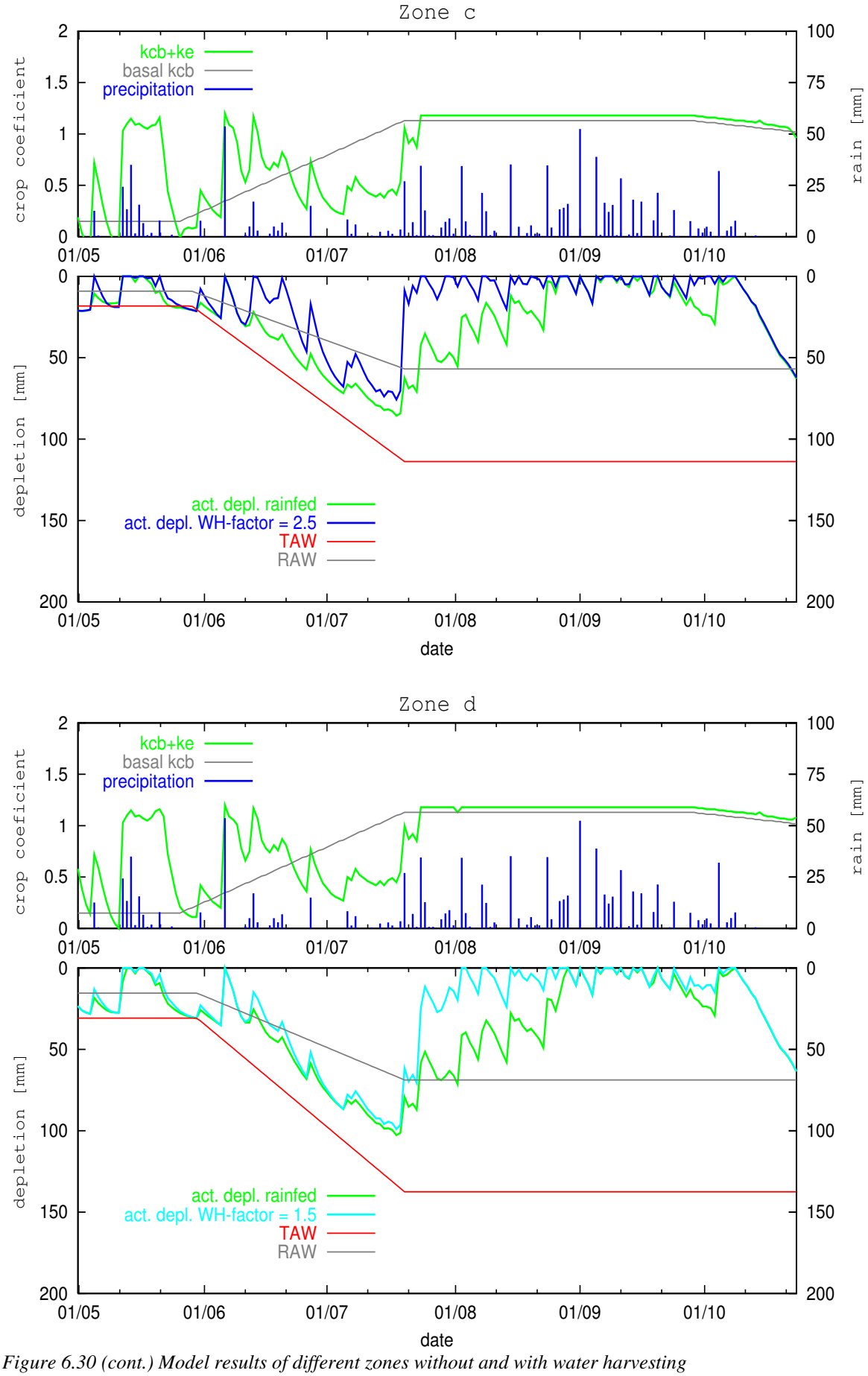

Figure 6.30 (cont.) Model results of different zones without and with water harvesting

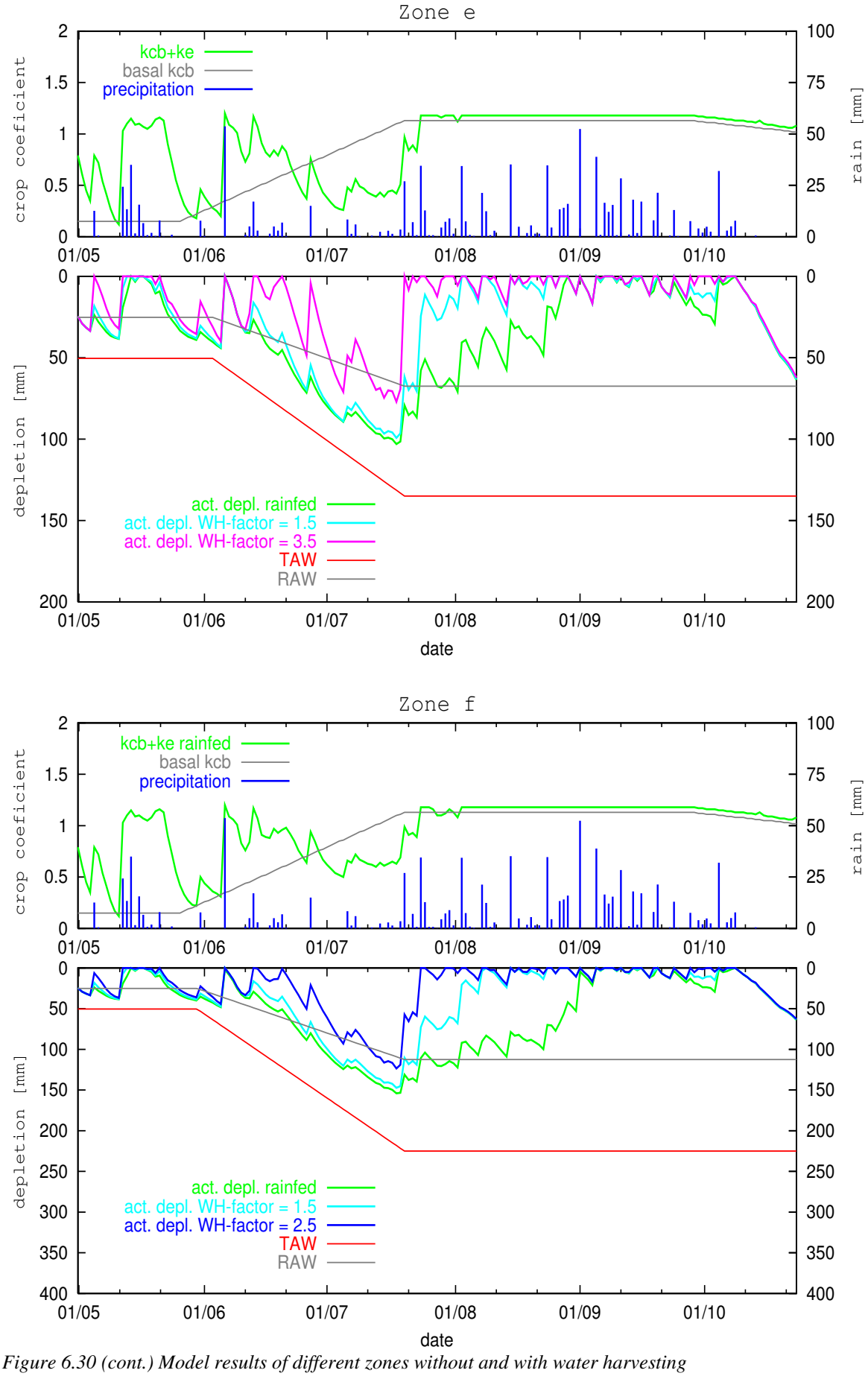

Figure 6.30 (cont.) Model results of different zones without and with water harvesting

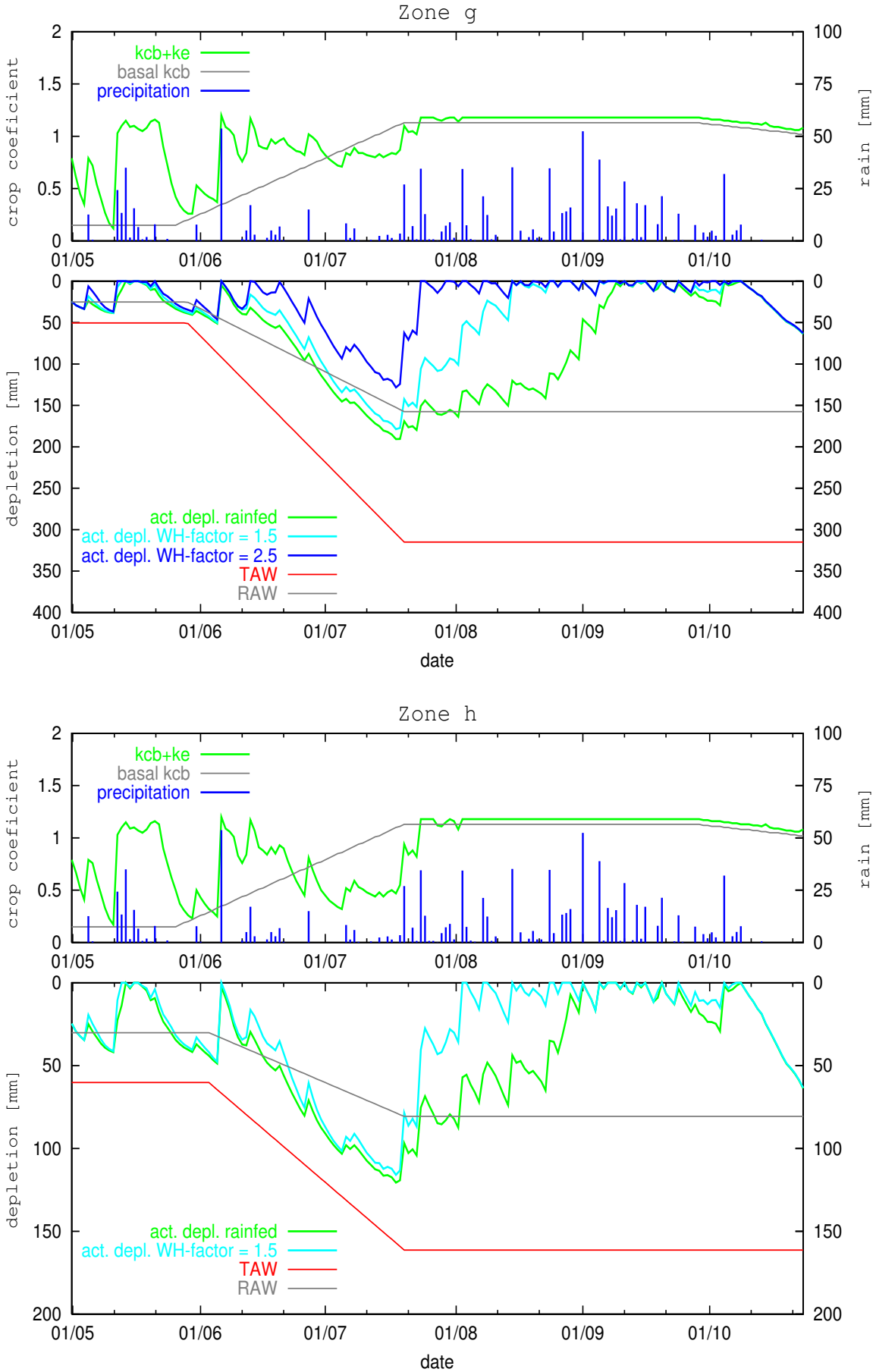

Figure 6.30 (cont.) Model results of different zones without and with water harvesting

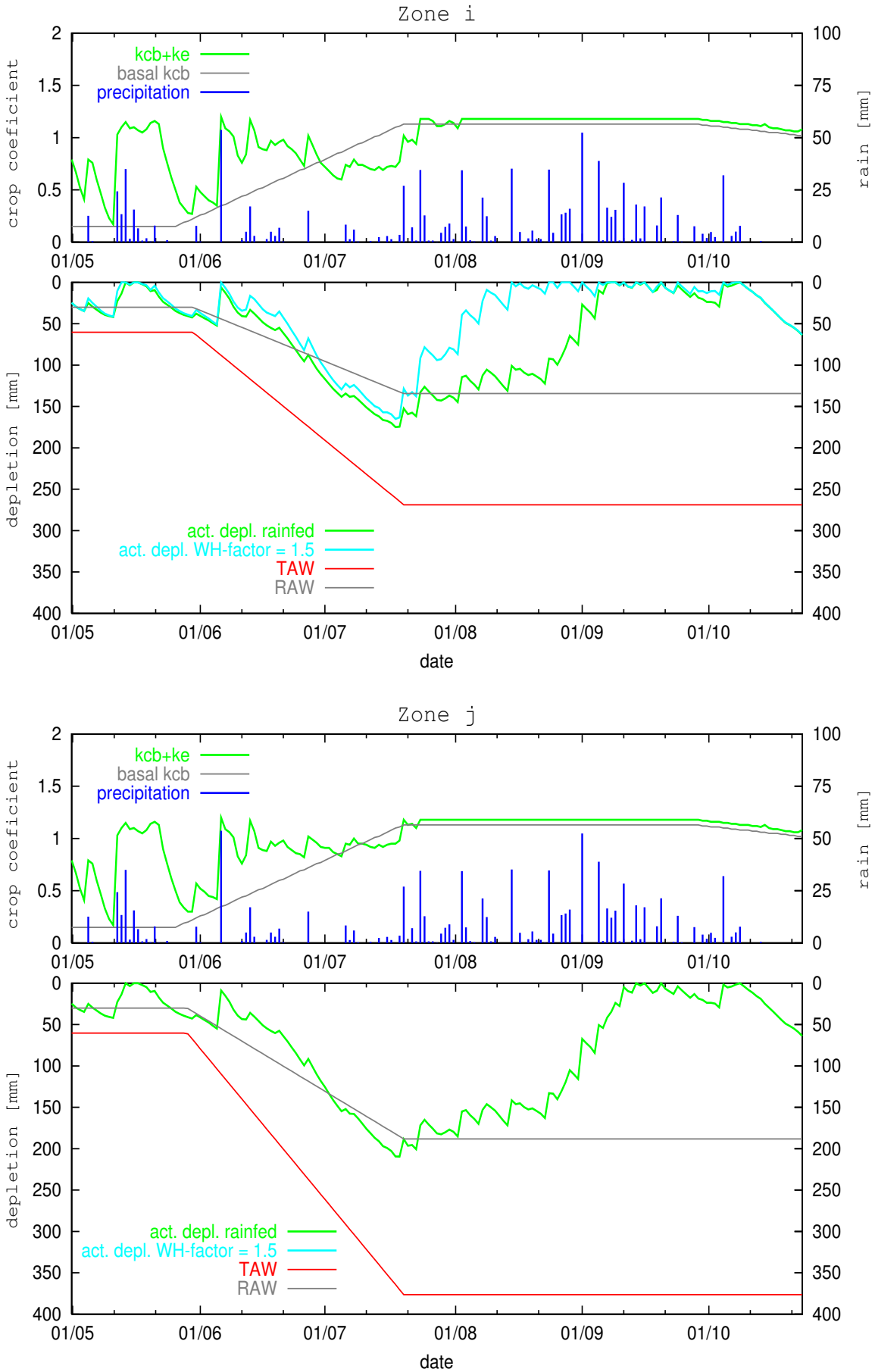

Figure 6.30 (cont.) Model results of different zones without and with water harvesting

6.3.2.3 The Effect of Thinning and Leaf Picking on the Water Consumption of Sorghum

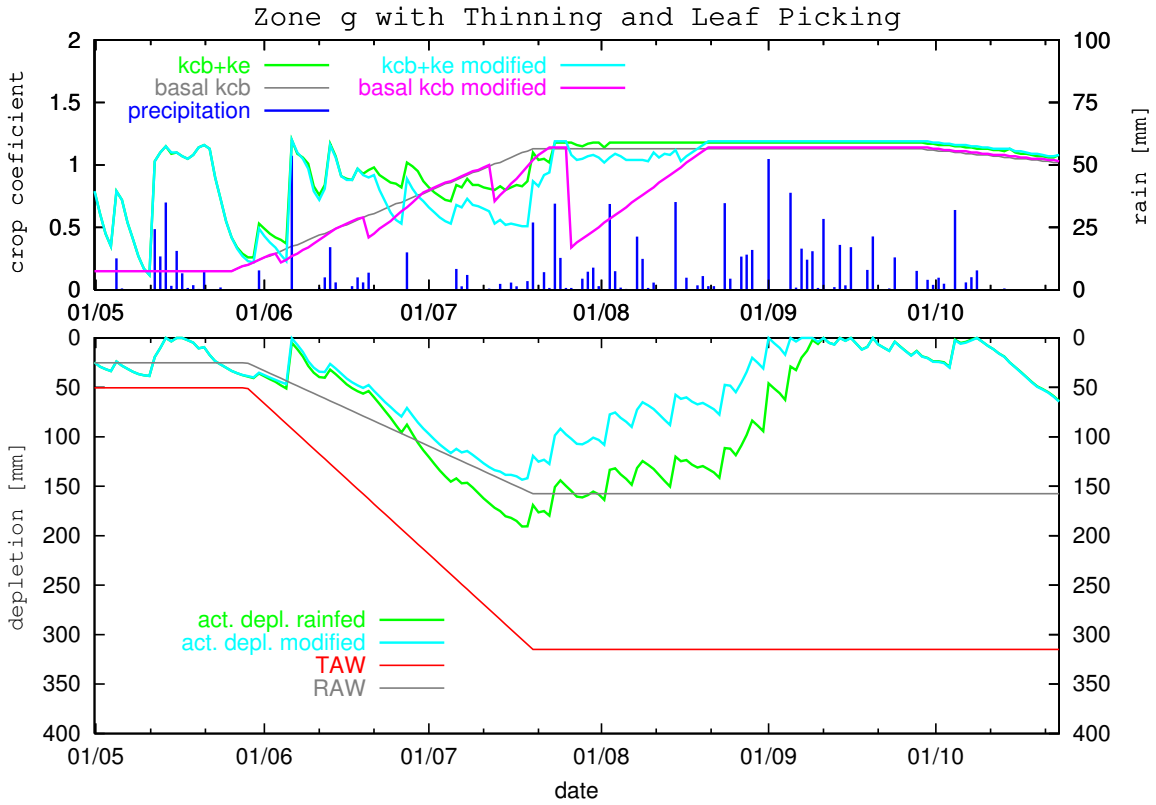

Figure 6.31 Example for the conceptional influence of thinning and leaf picking on the water consumtion of sorghum

The effect of “thinning” and “leaf picking” reduces the biomass and the leaf area index. With the thinning a number of plants on the field are completely taken out, while with the leaf picking commonly the majority of the leaves are picked and 4–8 leaves remain on the sorghum plant. The important difference between the two measures is that the thinning leaves the remaining plants untouched while the leaf picking affects interfere with every plant by reducing the number of leaves. There is no quantitative research known to the author on the water saving effects of these management methods. Therefore these modelling results are conceptual. The thinning is implemented in the model as a reduction of the basal crop coefficient by 30 % on the day of thinning, and a linear rise back to the normal basal crop coefficient within 10 days. Leaf picking, considered as the stronger impact, reduces the basal crop coefficient by 70 % and the linear rise takes 25 days. These values are related to the withdrawal of biomass. At the moment they are only hypothetical

assumptions because there are no reliable measurements on the dry matter biomass removal available. The dates of thinning are 4th June, 20th June, 13th July, the date of leaf picking is 27th July. The results are depicted for the class *g* in figure 6.31.

The graph of the modified basal crop coefficient shows clearly the sharp decline on the days of intervention by thinning and leaf picking. The effect on the dual crop coefficient is smaller but clearly remarkable in the case of thinning. The leaf picking during the wet mid-season stage shows only a very small reduction of the basal crop coefficient. Due to frequent rainfalls in the mid-season stage, the evaporation coefficient rises and compensates the partly the reduction achieved by the basal crop coefficient. This causes the dual crop coefficient to remain at a high level after the leaf picking. The modified depletion reduces the withdrawal sometimes by more than 60 mm. No water stress occurs during the whole growing season.

Although this is only a hypothetical model the result is remarkable because the reduction of the water requirements is only a side effect of these measures. The major factor which determines the efficiency of this kind of measures is the timing. The ideal moment would be at the beginning of a dry period which is of course not predictable. Therefore the thinning during the relatively dry development stage appears more appropriate in timing than the leaf picking in the wet mid-season. Nevertheless the leaf picking would save more water if rainfall was more scarce. Although it is not empirically proven these traditional measures seem to reduce the plant water requirements to a significant extent. In contrast to water harvesting, which enhances the water supply, the thinning and leaf picking reduce the water consumption and therefore provides an appropriate measure for water saving.

6.3.2.4 General Conclusion from the Modelling Scenarios

The modelling of the evapotranspiration using the dual crop coefficient shows the relation between precipitation, water harvesting factor, dry periods and total water storage capacity. The latter determines in combination with the rooting depth, the total available water (*TAW*). The fundamental fact regarding rainfed irrigation with or without water harvesting is that the timing and amount of water can not be specified. These agricultural

systems rely on the natural occurrence of rain. The possibility to overcome dry periods is related to the total storage capacity of the plant accessible soil water. This can be influenced by the terrace construction and, to a much lower extent and on a longer time scale, by soil management which increases the storage capacity (e. g. reduction of high stone content to enhance soil storage). The total available water determines the maximum period which can be overcome without water stress. This can be seen in the initial stage, where the rooting depth is small (0.2 m) and the differences between the zones and between the scenarios are also small.

When the *TAW* is determined, the following question is if rain occurs in sufficient quantity and frequency to supply enough water to keep the depletion between saturation and readily available water (*RAW)* level. All diagrams in figure 6.30 show that depletion crossed the *RAW*-level in all zones several times during the initial stage. Although water harvesting increases the length of the periods without water stress (the number of days with water stress decreases, see figure 6.29a), the maximum length of dry periods which can be covered is determined by the limited storage capacity rather than by the supplied rainfed irrigation.

The effect of water harvesting is stronger at the development stage and the mid-season stage. The development stage coincides with the intermediate dry season and depletion is the main process. The total available water benchmark increases and the water harvesting is more effective. Figure 6.29b shows a high number of days with water stress in the rainfed scenarios. Zones with limited water storage capacity ($a - e$) suffer almost the entire stage from water stress. However also the zones with higher water storage capacity ($f - j$) suffer from limited water availability during more than half of the period. The water harvesting scenario improves the water availability in contrast to the rainfed scenario significantly. Furthermore, also the magnitude of the water harvesting factor is relevant for the number of days with water stress. Nevertheless the water availability remain critical over a large period of the development stage. This stage appears to be the most critical one because insufficient water supply during the crop development endanger the crop mature in particular.

At the mid-season stage another effect of water harvestingcan be observed. Due to the scarce rain in the development stage the soil storage is low in the beginning of the mid-season stage and gets recharged by the ample rainfall of the mid-season stage. This situation permits studying the recharge behaviour of the different zones under wet conditions. At this stage the beneficial effect of water harvesting is good to recognise in the diagrams of figure 6.30. Under such circumstances also small water harvesting factors have relevant effect on the course of the graphs. The *RAW*-benchmark is crossed soon in all zones and in both scenarios, therefore the reduction of days with water stress (figure 6.29) is not that important as in the previous stages.

Agricultural management techniques like “thinning” and “leaf picking” are the complementary measures to water harvesting. They actively reduce the water consumption of the plants. The exemplary scenario is still hypothetical since the influence of biomass reduction on the basal crop coefficient is not proven. But the results are challenging. Under the given assumptions no water stress occurs.

The 1998 growing season showed that although the total rainfall was very high water scarcity appeared at the beginning of the growing season when precipitation remained rare. Water harvesting was not able to reduce this shortage completely although in the development stage it showed a significant improvement. In the later season, when high and frequent rainfall caused sufficient rainfed conditions, water harvesting caused an acceleration of the soil water recharge process.